L911174-11

N73-11437

DEVELOPMENT OF HIGH TEMPERATURE FASTENERS USING DIRECTIONALLY SOLIDIFIED EUTECTIC ALLOYS

FINAL REPORT

Contract NAS8-27358

AUGUST 23, 1972

Prepared for

George C. Marshall Space Flight Center
National Aeronautics and Space Administration
Marshall Space Flight Center, Alabama 35812

Prepared by:

F.D. George
Project Manager

Approved by:

E.R. Thompson, Chief
Advanced Metallurgy

United Aircraft
Research Laboratories

UNITED AIRCRAFT CORPORATION

EAST HARTFORD, CONNECTICUT 06108

United Aircraft Research Laboratories

UNITED AIRCRAFT CORPORATION

EAST HARTFORD, CONNECTICUT

Report L911174-11

DEVELOPMENT OF HIGH TEMPERATURE FASTENERS USING DIRECTIONALLY SOLIDIFIED EUTECTIC ALLOYS

FINAL REPORT

Contract NAS8-27358

August 23, 1972

Prepared for

George C. Marshall Space Flight Center
National Aeronautics and Space Administration
Marshall Space Flight Center, Alabama 35812

ABSTRACT

In a number of laboratories, directionally solidified eutectics are being examined as candidate materials for vanes and blades in advanced gas turbines. Because of the superior high temperature properties displayed by two such alloys, a program was initiated to determine the suitability of these materials for high temperature fasteners.

Material properties pertinent to fastener applications were determined as a function of temperature. These properties included shear parallel and perpendicular to the growth direction and torsion parallel to the growth direction. Several techniques were investigated for fabricating typical fastener shapes. These fabrication methods included grinding, creep forming and direct casting. Finally, a brief evaluation of the performance of the best fabricated fastener design was made.

Report L911174-11

Development of High Temperature Fasteners Using Directionally Solidified Eutectic Alloys

TABLE OF CONTENTS

LIST OF TABLES

LIST OF TABLES (Cont'd)

INTRODUCTION

In recognition of the current and anticipated requirements for superior high temperature materials, the Materials Laboratory of United Aircraft Research Laboratories has directed a substantial research effort in the establishment and evaluation of a technology for growing phase-reinforced eutectic alloys. The techniques used have demonstrated that materials with superior mechanical properties can be processed by the directional solidification of high temperature eutectic alloys. These investigations were prompted for the main purpose of developing an alloy for use in high temperature turbine applications. Several nickel and cobalt-based, phase-reinforced composite systems have been identified which display superior mechanical properties for temperatures to 2200°F. Certain of the characteristics, notably microstructural stability, tension, creep and fatigue, suggested that these type materials might qualify as high temperature fasteners for attaching thermal protection panels on space vehicles. For example, good microstructural stability would assure non-weakening of the fastener head area at the working temperatures and high creep resistance would prevent relaxation under load and help retain a "tight joint".

In comparison with other composite techniques for obtaining superior high temperature materials, the directionally solidified eutectic approach offers numerous advantages. One of the most important advantages is that a eutectic composite develops its reinforcing phase in situ by a one-step casting process. Since the composite structures are generated as a result of an equilibrium reaction, the phases produced are chemically stable with respect to one another. Furthermore, experience has shown that the low energy interfaces, established during the growth, result in a microstructure with exceptional stability which resists coarsening and spheroidization. Mechanically, as a first approximation, the behavior of these materials can be treated as normal composites. Recently it has been shown, however, that there is an portant effect of interphase spacing on strength. Reducing this spacing, which is accomplished by growing the material at a faster rate, has strengthened the material according to a Hall-Petch relationship. Thus, not only is processing benefited by rate increases but also properties.

Included in the disadvantages in the eutectic approach are anisotropic properties (as with other composites), a general inability to vary randomly the volume fraction of the phases, and some lack of freedom in selection of interesting systems. These last two disadvantages occur because we have selected to use a eutectic or eutectic-like composition where two or more phases crystallize simultaneously from a liquid. Even within these limitations, there are countless systems which can be anticipated if one considers ternary and higher order systems for study and development.

The prime material evaluated in this study was the directionally solidified Ni_3Al-Ni_3Cb eutectic alloy (Refs. 1-5). After solidification the microstructure consists of a lamellar (sheet-like) dispersion of Ni_3Cb within a Ni_3Al matrix (Fig. 1). It contains approximately 44 volume percent of the Ni_3Cb reinforcing phase, and the Ni_3Al matrix (a ductile intermetallic compound) is strengthened substantially by the 8 at. % columbium dissolved within it. The eutectic melting temperature is 2335°F and its density is 8.5 gm/cc. The alloy is a high modulus material whose tensile strength and creep-rupture strength are markedly superior to conventional superalloys. It is mildly notch sensitive at room

temperature but is notch insensitive at elevated temperatures. Although it possesses low tensile ductility at room temperature, this does not mean the material is brittle. Its toughness is, in fact, comparable to superalloys at room temperature. The fatigue strength of the alloy is outstanding at room temperature, greatly surpassing that of nickel superalloys. This eutectic alloy exhibits such remarkable properties by virtue of the directional nature of its microstructure. The properties of the material are, as a consequence, directional. This material offers interesting possibilities for application as a high temperature fastener and if successfully developed, should satisfy performance requirements which cannot be met by conventional materials.

Since the Ni_3Al-Ni_3Cb alloy is representative of only one class of eutectic composites, i.e. the lamellar reinforced, a limited evaluation of the (Co,Cr)-$(Cr,Co)_7C_3$ eutectic (Refs. 6-8) which is representative of the fibrous reinforced eutectic composite was also included in this program. This cobalt-based eutectic was modified by the addition of aluminum for the purpose of improving its oxidation resistance and to aid in stabilizing the cubic form of the cobalt in the alloy. The microstructure of this alloy is fibrous in nature (Fig. 1) and consists of 26 volume percent of the carbide reinforcing phase with a cobalt, chromium, aluminum solid solution matrix. It has a density of 8.0 gm/cc and a melting temperature of 2370°F. Although not as strong as the Ni_3Al-Ni_3Cb eutectic alloy, the (Co,Cr,Al)-$(Cr,Co)_7C_3$ eutectic is more easily grown - rates of 50 cm/hr are typical - and is more oxidation resistant than the Ni_3Al-Ni_3Cb eutectic. This alloy is stronger than the conventional cast nickel-base superalloys in tension and creep and has comparable impact toughness. Because of the presence of the aligned fibrous carbide phase, it displays a high elastic modulus at room and elevated temperatures.

Other examples of "exotic" alloys which have been selected for study as candidate materials for potential use as high temperature structural fasteners include a dispersion strengthened metal TD NiCr (Ref. 9) and these evaluations will be used for comparison purposes where possible.

EXPERIMENTAL PROCEDURES

Melting and Solidification

Master melts of eutectic composition were made in alumina crucibles and chill-cast in copper molds. The resulting bars were then placed in 1.27 cm (1/2 in.) diameter 99.7 percent recrystallized alumina cylindrical crucibles and unidirectionally solidified vertically within a resistively heated graphite tube furnace under a dynamic argon atmosphere (Fig. 2). These crucibles were held in a graphite sleeve which separated the crucible bottom from a water cooled brass pedestal by .64 cm (1/4 in.) of graphite. The crucibles were lowered from the furnace at rates corresponding to a nominal* solidification velocity of 2 cm/hr (0.79 in./hr) for the Ni_3Al-Ni_3Cb eutectic and 10 cm/hr (3.95 in/hr) for the (Co,Cr,Al)-$(Cr,Co)_7C_3$ eutectic. Liquid superheats of approximately 260°C (500°F) were employed and the thermal gradient in the liquid was estimated to have been 70°C/cm. Several 1.27 cm (1/2 in.) diameter ingots of both materials were formed as cast products by this vertical Bridgman-type directional solidification process. These ingots were then ground into test samples for the determination of the material properties pertinent to fastener application.

Evaluation of Properties

Transverse Shear

Bar samples rectangular in cross-section, 0.32 cm x 0.64 cm x 2.54 cm (1/8 in. x 1/4 in. x 1 in.), were ground from these ingots with the direction of solidification parallel to the longest dimension so the strength in shear perpendicular (transverse) to the growth direction might be measured. The double shear test fixtures used to measure the transverse shear are shown in Figs. 3 and 4. The metal alignment fixture with hardened steel loading faces (Fig. 3) was designed and fabricated in order to investigate the effects of varying spans (single shear distances between the punch and anvil) at room temperature and also to allow the sample ends to be clamped. The alumina fixture (Fig. 4) was used for some room temperature tests but was primarily used in the higher temperature tests. All transverse shear tests were performed in air at a loading rate of 0.025 cm/min (0.01 in./min) using a Tinius-Olsen four-screw machine.

Longitudinal Shear

Test specimens of both eutectic alloys for measuring longitudinal shear strength, shear parallel to the direction of solidification, were ground to shape and tested. These specimens consisted of a 0.64 cm (1/4 in.) diameter bolt shank with two 0.32 cm (1/8 in.) thick heads (one at each end of the shank) which were attached to a fixture (Fig. 5) composed of two high temperature

*The failure to develop an exactly uniform rate of growth is primarily the result of the changing thermal gradient in the solid.

slotted button-head adapters and split ring washers (to assure full bearing on the specimen heads). All longitudinal shear tests were run in air at a loading rate of 0.025 cm/min (0.01 in./min) using a Tinius-Olsen four-screw machine.

Longitudinal Thread Shear

Longitudinal thread shear specimens 5 cm (2 in.) long with 1/4-20 threads at either end were ground from both eutectic ingots with the direction of solidification parallel to the long dimension. These specimens were tested in a fixture which is shown schematically in Fig. 6. All thread shear tests were run in air at a loading rate of 0.025 cm/min (0.01 in./min) using a Tinius-Olsen four-screw machine.

Torsion

Solid rod samples with gage sections of 0.318 cm (0.125 in.) diameter and either 5 cm (2 in.) or 2.5 cm (1 in.) long, with the long axis parallel to the growth direction, of both the Ni_3Al-Ni_3Cb and (Co,Cr,Al)-$(Cr,Co)_7C_3$ alloys were fractured in torsion using the test apparatus shown in Fig. 7. This apparatus was satisfactory for use in determining the torsional strength of the eutectic alloys at room temperature and at 204°C (400°F). By substituting an induction heating source (Fig. 8) for the resistance furnace, tests were also satisfactorily run at temperatures up to 1204°C (2200°F). The high temperature tests were accomplished, without the necessity of cooling the test adapters, by increasing the overall length of the test samples from 11.5 cm (4 5/8 in.) to 15 cm (6 in.) and reducing the length of the gage section from 5 cm (2 in.) to 2.5 cm (1 in.). The strain was measured by a time scale which was converted to an angle of twist measurement. In a few low temperature tests, where the shear modulus was determined, the strain was measured by bonded strain gages [maximum short time useful temperature of 204°C (400°F)] oriented in the direction of the principal stress. The rate of applied torque was .67 RPM.

Fabricating Techniques

Grinding

All the test specimens for determining the material properties pertinent to fastener application of both eutectic alloys were fabricated by grinding. Several double flush headed specimens [shank diameter = 0.635 cm (0.250 in.)] were ground to shape, with the direction of solidification parallel to the long axis of the specimen, from Ni_3Al-Ni_3Cb ingots for use in evaluating this process as a method for fabricating fasteners.

Casting

A few single and double 100° flush headed specimens with 0.635 cm (0.250 in.) diameter shanks of the Ni_3Al-Ni_3Cb eutectic were directionally cast parallel to the long axis of the specimen in order to evaluate this process as a method of fabricating fasteners. This technique required the use of high purity alumina foundry fabricated molds in the apparatus previously described and shown in Fig. 2.

Creep Forming

Bar samples [0.635 cm (0.250 in.) diameter by approximately 4.3 cm (1.7 in.) long] of both eutectics were ground with the direction of solidification parallel to the long dimension. These bar samples of both alloys were creep formed into flush head fastener shapes using a molybdenum die. The forming was accomplished in vacuum at 1204°C (2200°F) at a rate of approximately 0.038 cm per min (0.015 in. per min) and a pressure of approximately 172 x 10^6 N/m^2 (25 x 10^3 psi). The 100° flush head formed was 1.02 cm (0.40 in.) in diameter and 0.15 cm (0.06 in.) high. Several specimens were fabricated in this manner to determine the shear strength of these eutectic materials when made into a typical fastener shape using the creep forming process.

Evaluation of Fabricated Fasteners

A 100° countersunk flush head design was chosen as a typical fastener shape for the evaluation of fabricated fasteners because this configuration is common in the assembly of skin panels to substructures where a flush surface is required.

Room Temperature Shear Strength

Several room temperature shear strength tests of 100° flush head fastener shapes of the Ni_3Al-Ni_3Cb eutectic made from the three fabrication techniques were performed. The double headed specimen configurations were tested in the same manner as described in the longitudinal shear strength determinations and shown in Fig. 5. The single headed fastener configurations were tested using a V-type wedge grip with serrated faces which clamped around the shank of the fastener. Figure 9 shows a schematic of the single flush head test fixture used. A few creep formed (Co,Cr,Al)-$(Cr,Co)_7C_3$ eutectic specimens were also tested for comparison. The specimens tested were fabricated with the direction of solidification parallel to the long axis of the fastener shape. All of the shear strength tests were run in air at a loading rate of 0.025 cm/min (0.01 in./min) using a Tinius-Olsen four-screw machine.

Effect of Flush Head Angle on Room Temperature Shear Strength

Double flush headed specimens of the Ni_3Al-Ni_3Cb eutectic which were ground to shape, were tested to determine the effective longitudinal shear strength (shear parallel to the direction of solidification) at room temperature of this material as a function of flush head angle. These double headed specimens were also tested in air at a loading rate of 0.025 cm/min (0.01 in./min) using a Tinius-Olsen four-screw machine in the same manner as described in the longitudinal shear strength determinations.

Effect on Room Temperature Torsional Strength after Exposure at 2200°F

Directionally solidified ingots of both the Ni_3Al-Ni_3Cb and (Co,Cr,Al)-$(Cr,Co)_7C_3$ eutectics were prepared and ground into torsion specimens for room temperature torsional tests after exposure at 1204°C (2200°F) for 30, 60, and 120 minutes. These solid rod specimens with a 0.318 cm (0.125 in.) diameter

by 2.5 cm (1 in.) long gage section were ground to shape with the long axis parallel to the growth direction. The strain was measured by a time scale which was converted to an angle of twist measurement. The rate of applied torque was .67 RPM. The test apparatus was the same as that used in the torsional strength determinations (Fig. 7).

Shear Rupture

Directionally solidified ingots of the Ni_3Al-Ni_3Cb eutectic alloy were prepared and ground into double headed longitudinal shear specimens for short-term stress-rupture testing. The specimen and adapter designs used were the same as described in the longitudinal shear strength determinations. These tests were carried out in air under a constant load at 816°C (1500°F) and 1093°C (2000°F).

RESULTS AND DISCUSSION

Material Property Evaluation Pertinent to Fastener Application

Transverse Shear

A double shear test fixture was used in this evaluation and initially the effect of span variations and the effect of the sample ends being clamped or free on the room temperature transverse shear strength were determined. The effect of span variations on the room temperature transverse shear strength of the Ni_3Al-Ni_3Cb eutectic is shown in Fig. 10. The high shear strength measured at the 0.025 cm (0.010 in.) span was due in part to the support of the sample by the anvil whereas the samples tested at the 0.185 cm (0.073 in.) span appeared to have failed partly in bending which may explain the lower apparent shear strength measured. The samples tested at the intermediate span distances appeared to have failed in shear and the mean value was considered as the effective shear strength of the material at room temperature. An increase in shear strength is indicated at the 0.185 cm (0.073 in.) span when the sample ends were clamped (Fig. 10). However, there appears to be little effect due to clamping at the intermediate spans where shear failures were observed. Because of this and the temperature limitation of the metal clamping fixture, all high temperature tests were run with free ends at a constant span within this intermediate range. Table I summarizes the results of the effect of temperature on the transverse shear strength of the Ni_3Al-Ni_3Cb eutectic.

The effective transverse shear stress vs. deflection curves for the Ni_3Al-Ni_3Cb eutectic alloy at various span distances are shown in Fig. 11. The initial sample tested at 1204°C (2200°F) exhibited a large amount of deformation which caused jamming and eventual fracture of the alumina punch and anvil. This behavior is reflected in the shape of the stress-deflection curve (Fig. 11) where an increase in stress occurred after an obvious deviation from linearity at 75 x 10^6 N/m^2 (10.9 x 10^3 psi). All subsequent high temperature tests were terminated following the initial deviation from linearity and this value was considered as the effective transverse shear strength of the material at that particular temperature.

In Fig. 12, a plot of effective shear stress vs. temperature indicates that the transverse shear strength of the Ni_3Al-Ni_3Cb eutectic is insensitive to temperature up to 538°C (1000°F). As shown by the specimens pictured in this figure, the transversely oriented Ni_3Al-Ni_3Cb displayed increasing ductility with temperature.

The effect of span variations on the room temperature transverse shear strength of the (Co,Cr,Al)-$(Cr,Co)_7C_3$ eutectic is plotted in Fig. 13. Although the resulting room temperature shear strengths are higher than for the Ni_3Al-Ni_3Cb eutectic, this alloy exhibits a similar response to span and clamping for spans between 0.050 and 0.200 cm. Therefore, as in the previous case, all high temperature tests were run with free ends at a constant span within this intermediate range.

Table I

Transverse Shear Strength of Ni_3Al-Ni_3Cb
Eutectic Solidified at 2 cm/hr

Specimen Number	Temperature		Span		Shear Strength	
	°C	(°F)	cm	(in.)	10^6 N/m^2	(10^3 psi)
A70-593-3*	24	(75)	0.025	(0.010)	828	(120.0)
A71-337-4*	24	(75)	0.051	(0.020)	576	(83.5)
A71-397-01A**	24	(75)	0.051	(0.020)	636	(92.2)
A70-593-1	24	(75)	0.107	(0.042)	528	(76.5)
A71-337-1	24	(75)	0.107	(0.042)	531	(77.0)
A71-337-2	24	(75)	0.107	(0.042)	479	(69.5)
A71-337-3*	24	(75)	0.107	(0.042)	576	(83.5)
A70-593-2	24	(75)	0.185	(0.073)	328	(47.5)
A71-397-01B	24	(75)	0.185	(0.073)	315	(45.7)
A71-463-01*	24	(75)	0.185	(0.073)	446	(64.6)
A71-398-01	260	(500)	0.074	(0.029)	569	(82.5)
A71-398-02	260	(500)	0.074	(0.029)	568	(82.3)
A71-398-03	538	(1000)	0.074	(0.029)	580	(84.1)
A71-398-04	538	(1000)	0.074	(0.029)	548	(79.4)
A71-463-02	538	(1000)	0.076	(0.030)	609	(88.3)
A71-398-05	816	(1500)	0.074	(0.029)	457	(66.2)
A71-398-06	816	(1500)	0.074	(0.029)	473	(68.5)
A71-398-07	1093	(2000)	0.076	(0.030)	142	(20.6)
A71-398-08	1093	(2000)	0.076	(0.030)	190	(27.6)
A71-463-03	1093	(2000)	0.076	(0.030)	172	(24.9)
A70-593-4	1204	(2200)	0.074	(0.029)	75	(10.9)
A71-398-09	1204	(2200)	0.076	(0.030)	72	(10.5)

Loading rate = 0.025 cm/min (0.01 in./min)
Sample ends free (alumina fixture - Ref. Fig. 4)
*Sample ends clamped (metal fixture - Ref. Fig. 3)
**Sample ends free (metal fixture - Ref. Fig. 3)

The results obtained in the determination of the effect of temperature on the shear strength of the (Co,Cr,Al)-$(Cr,Co)_7C_3$ eutectic are summarized in Table II.

Table II

Transverse Shear Strength of (Co,Cr,Al)-$(Cr,Co)_7C_3$
Eutectic Solidified at 10 cm/hr

Specimen Number	Temperature		Span		Shear Strength	
	°C	(°F)	cm	(in.)	10^6 N/m^2	(10^3 psi)
A71-504A-01*	24	(75)	0.025	(0.010)	794	(115.0)
A71-504C-02**	24	(75)	0.025	(0.010)	780	(113.0)
A71-418A**	24	(75)	0.051	(0.020)	721	(104.5)
A71-504B-01*	24	(75)	0.051	(0.020)	780	(113.0)
A71-418B**	24	(75)	0.076	(0.030)	686	(99.5)
A71-504C-01*	24	(75)	0.076	(0.030)	704	(102.0)
A71-504C-05**	24	(75)	0.185	(0.073)	455	(66.0)
A71-504B-02	260	(500)	0.076	(0.030)	590	(85.5)
A71-504C-03	260	(500)	0.076	(0.030)	566	(82.0)
A71-504A-02	538	(1000)	0.076	(0.030)	559	(81.0)
A71-504B-03	538	(1000)	0.076	(0.030)	529	(76.7)
A71-504A-03	816	(1500)	0.076	(0.030)	242	(35.0)
A71-504B-04	816	(1500)	0.076	(0.030)	242	(35.0)
A71-504A-04	1093	(2000)	0.076	(0.030)	68	(9.9)
A71-504C-04	1093	(2000)	0.076	(0.030)	68	(9.9)
A71-504A-05	1204	(2200)	0.076	(0.030)	40	(5.8)
A71-504B-05	1204	(2200)	0.076	(0.030)	41	(6.0)

Loading Rate = 0.025 cm/min (0.01 in./min)
Sample ends free (alumina fixture - Ref. Fig. 4)
*Sample ends clamped (metal fixture - Ref. Fig. 3)
**Sample ends free (metal fixture - Ref. Fig. 3)

The effective transverse shear stress vs. deflection curves for the (Co,Cr,Al)-$(Cr,Co)_7C_3$ eutectic alloy at various span distances are shown in Fig. 14. As in the Ni_3Al-Ni_3Cb eutectic, the stress-deflection curve for the sample tested at 1204°C (2200°F) exhibited an increase in stress after a deviation from linearity. The stress prior to this increase has been considered as the effective transverse shear strength of the material at that particular test temperature.

The temperature dependence of transverse shear strength of the (Co,Cr,Al)-$(Cr,Co)_7C_3$ material is shown in Fig. 15. This eutectic shows only a slight decrease in shear strength up to 538°C (1000°F) and at that temperature exhibits a shear strength equivalent to that observed for the Ni_3Al-Ni_3Cb eutectic. Above this temperature, the shear strength drops off rather rapidly. The test specimens in Fig. 15 also show an increasing ductility with temperature.

The temperature dependence of the transverse shear strength of both eutectic alloys is shown in Fig. 16 along with the shear strength values determined for 0.64 cm (1/4 in.) diameter specimens of TD NiCr (Ref. 9) based on double shear testing. This dispersion strengthened metal which had been selected for study as a candidate material for potential use as a high temperature fastener yielded values that closely compare with those obtained for the fibrous (Co,Cr,Al)-$(Cr,Co)_7C_3$ eutectic.

Longitudinal Shear

Initially, bolt samples [1/4-20 thread x 5 cm (2 in.) long] for measuring longitudinal shear strength, shear parallel to the direction of solidification, were ground to shape and tested at room temperature. The bolt heads were 0.32 cm (1/8 in.) in height with their bearing surfaces perpendicular to the shank of the bolt, while the average head to shank radius was 0.046 cm (0.018 in.). These preliminary longitudinal shear strength results are given in Table III and the fractured specimens are shown in Fig. 17.

Table III

Room Temperature Longitudinal Shear Strength of Ni_3Al-Ni_3Cb Eutectic

Specimen Number	Solidification Rate		Shear Strength		Failure
	cm/hr	(in./hr)	$10^6 N/m^2$	(10^3 psi)	
A70-593H	2.0	(0.79)	174	(25.2)	Complete head shear (Fig. 17a)
A71-337T	2.0	(0.79)	>177	(>25.7)	Thread (Fig. 17c)
A71-403T	2.8	(1.10)	224	(32.4)	Thread & partial head shear (Fig. 17b)

Loading rate - 0.025 cm/min (0.01 in./min)

The longitudinal shear strength values were determined using the diameter of the bolt shank in calculating the shear area. This approximation was used because the actual sheared area, as seen in Fig. 17a where complete head shear failure was experienced, was not perfectly cylindrical which probably reflects the effect of the different orientations of the lamellae in the various grains sheared.

The test on specimen number A71-337T which resulted in thread failure (Fig. 17c) corresponds to the ASTM specifications (A370) for axial tension testing on full size bolts. The specifications require the bolt to be tested in a holder with the load axially applied between the head and a nut or suitable fixture and the tensile failure to occur in the body or threaded section with no failure at the junction of the body and head. The stress area is to be calculated from the mean of the mean root and pitch diameters of class 3 external threads as shown in the following equation.

$$A_s = 0.7854\ (D - 0.9743/n)^2$$

where A_s = stress area
D = nominal diameter
n = number of threads per inch

Using this equation to calculate the stress area and knowing the load at failure, the axial tensile strength of the bolt at room temperature was found to be approximately 85,500 psi. Assuming the room temperature unnotched tensile strength of this eutectic alloy grown at 2 cm/hr to be 170,000 psi (Ref. 1) then the stress concentration caused by the presence of the threads yields a notched strength ratio of 0.50. This sensitivity at room temperature was shown previously (Ref. 1) where a concentric notch resulted in a notched strength ratio of approximately 0.65.

Many contributing factors were assumed to reflect on these longitudinal shear strength results obtained. Some of these variables such as head to shank radius, microstructure, grain size, and the horizontal span between the shank of the bolt and the bearing surface of the fixture at the head were examined. Of the three specimens tested, all the microstructures appeared to be relatively similar. Microstructural examination showed that the specimens were composed of well aligned lamellar grains with no observable defects. However, the head to shank radii and the horizontal spans were different in each specimen. Also, the grain size, which is affected by solidification method and rate, appeared to be finer in the A71-403T specimen.

Subsequent testing in the evaluation of the longitudinal shear strength of this eutectic alloy incorporated bolt heads of shorter height in order to cause shear failure in the head, and closer tolerances on the head to shank radius and the shank diameter. This, in conjunction with a new fixture that was designed and fabricated, allowed an investigation at room temperature of the effect of different shearing spans on the longitudinal shear strength.

Bolt samples [1/4-20 thread x 5 cm (2 in.) long] with head heights of about 0.170 cm (0.067 in.) were ground to shape and tested at room temperature at different shearing spans. The results obtained are given in Table IV.

Table IV

Room Temperature Longitudinal Shear Strength* of Ni_3Al-Ni_3Cb Eutectic Solidified at 2 cm/hr

Specimen Number	Span		Bolt Head Height		Shear Strength	
	cm	(in.)	cm	(in.)	10^6 N/m^2	(10^3 psi)
A71-397-02**	0.025	(0.010)	0.185	(0.073)	166	(24.0)
A71-491-03	0.025	(0.010)	0.160	(0.063)	215	(31.2)
A71-491-01	0.051	(0.020)	0.160	(0.063)	110	(15.9)
A71-491-02***	0.102	(0.040)	0.180	(0.071)	70	(10.2)
A71-397-03	0.153	(0.060)	0.170	(0.067)	79	(11.5)

Loading rate = 0.025 cm/min (0.01 in./min)
*Questionable data (for data considered reliable see Table VI)
**Several cracks evident in bolt head prior to testing
***Fractured specimen indicated possible precracked head

Precracking, caused by the grinding operation used to fabricate the thin bolt heads which were required to avoid tensile fracture, may have affected the results obtained. Prior to testing, examination of the bolt head of specimen number A71-397-02 with a dye penetrant process revealed several cracks. The sample was then tested and the resulting shear strength fell below the previous shear strength value obtained under similar test conditions. Therefore, due to the uncertainty regarding cracks prior to testing, the shear strength values listed in Table IV were disregarded.

Two approaches were initiated to assure reliable data in this study. The first involved a new test specimen design which has been used for determining shear strengths in aluminum/boron composites. An aluminum alloy (6061-T6) was chosen to evaluate this specimen design. The results obtained are given in Table V and the corresponding test specimen designs are shown in Fig. 18.

Table V

Room Temperature Shear Strength of 6061-T6

Spec. No.	Shear Area*		Shear Span*		Shear Strength		Failure
	cm^2	($in.^2$)	cm	(in.)	10^6 N/m^2	(10^3 psi)	
1*	0.203	(0.0315)	0.076	(0.030)	182	(26.4)	Shear[1]
2	0.205	(0.0318)	0.076	(0.030)	180	(26.1)	Shear[1]
3	0.204	(0.0316)	0.076	(0.030)	182	(26.4)	Shear[1]
4*	0.204	(0.0316)	0.076	(0.030)	217	(31.5)	Shear[2]
5*	0.201	(0.0311)	0.076	(0.030)	---	---	Bending[3]
6	0.202	(0.0314)	0.076	(0.030)	---	---	Tensile[3]
7	0.207	(0.0321)	0.076	(0.030)	---	---	Tensile[3]
8*	0.207	(0.0321)	0.076	(0.030)	---	---	Tensile[3]
9	0.100	(0.0155)	0.076	(0.030)	---	---	Tensile[3]
10	0.100	(0.0155)	0.076	(0.030)	---	---	Tensile[3]
11*	0.100	(0.0155)	0.076	(0.030)	---	---	Tensile[3]
12	0.100	(0.0155)	0.076	(0.030)	---	---	Tensile[3]
13	0.102	(0.0158)	0.038	(0.015)	206	(29.8)	Shear
14	0.102	(0.0158)	0.038	(0.015)	216	(31.3)	Shear
15	0.102	(0.0158)	0.038	(0.015)	213	(30.9)	Shear
16*	0.102	(0.0158)	0.038	(0.015)	215	(31.1)	Shear

*Ref. Fig. 18

[1]Sample ends free
[2]Sample ends clamped
[3]Mechanical restraint to prevent bending

The design of specimens numbered 1-4 was similar to that used in determining the transverse shear strength of the eutectic alloys. Although clamping the ends of specimen #4 (Fig. 18) caused an increase in shear strength, the resulting values for these 6061-T6 specimens (1-4) compare favorably with the average shear strength value given in the Metals Handbook (Ref. 10) for the same material.

Specimens numbered 5-16 are a progression of designs for the purpose of obtaining a shear failure in a design similar to the one which has been used for determining shear strengths in aluminum/boron composites and one which would be applicable in the longitudinal shear strength measurement for the eutectic alloys. Specimen #5 (Fig. 18) failed in bending; this was prevented in subsequent tests (specimens numbered 6-12) by the introduction of a mechanical restraint. However, all of these tests resulted in tensile failures (Ref. specimen numbers 8 and 11 in Fig. 18) even though the shear area was reduced in specimens numbered 9-12. Finally, in specimens numbered 13-16 the tensile area was increased by a factor of 3 and shear failures were produced (Fig. 18) with resulting shear strength values equivalent to the typical value given for the 6061-T6 alloy. This final design could create the same precracking problem experienced in the attempt to fabricate thin bolt heads. This might be avoided if, instead of a grinding operation, the slots were made by either an electrochemical or electrodischarge machining operation.

Since the bolt design samples of the eutectic have shown that thicker bolt heads cause failure in the root of the thread (Ref. Table III, Fig. 17b & c) and the thinner bolt heads experience cracking during fabrication, the second approach taken was to eliminate the threads completely and incorporate a test specimen having two relatively thick heads (one at each end of the shank). A typical test specimen attached to the longitudinal shear fixture, composed of two high temperature slotted button-head adapters and split ring washers (to assure full bearing on the specimen heads), was shown in Fig. 5. From the results given in Table IV, no conclusion could be drawn with respect to the effect of shearing span variation on the room temperature longitudinal shear strength of the Ni_3Al-Ni_3Cb eutectic. However, all specimens tested in that study exhibited shear failure and therefore a constant shearing span distance of 0.025 cm (0.010 in.) was chosen to be used in the following longitudinal shear strength determinations.

Although both specimen designs appeared satisfactory in yielding reliable shear strength values, the flat slotted specimen design (Fig. 18) was not considered further because of the anticipated fabrication problems previously mentioned. Therefore, the test specimen and test fixture design (Fig. 5) as explained in the second approach was used to complete the study of determining the temperature dependence of the eutectic material strength in shear parallel (longitudinal) to the growth direction. The results obtained are given in Table VI.

The temperature dependence of longitudinal shear strength of the Ni_3Al-Ni_3Cb alloy is shown in Fig. 19. An initial increase in longitudinal shear strength with an increase in temperature is evident. This increase is undoubtedly partly due to the increase in the flow stress of the Ni_3Al phase with temperature. This anomalous behavior has also been found in a $Ni_3(Al,Cb)$ single phase alloy, which is similar to the matrix phase of the eutectic, by Thornton, et al (Ref. 11). The yield strength of this intermetallic compound increases with temperature up to approximately 700°C (1292°F).

Table VI

Longitudinal Shear Strength of Ni_3Al-Ni_3Cb Eutectic Solidified at 2 cm/hr

Specimen Number	Temperature		Effective Shear Strength	
	°C	(°F)	10^6 N/m^2	(10^3 psi)
A71-465A-01	24	(75)	179	(25.9)
A71-465B-02	24	(75)	195	(28.2)
A71-516	24	(75)	189	(27.4)
A71-698A	260	(500)	218	(31.6)
A71-702A-01	260	(500)	209	(30.3)
A71-702B-01	260	(500)	215	(31.2)
A71-465A-02	538	(1000)	262	(38.0)
A71-494B	538	(1000)	212	(30.8)
A71-726-02	538	(1000)	198	(28.7)
A71-465B-01	816	(1500)	199	(28.8)
A71-494A	816	(1500)	217	(31.4)
A71-698C	816	(1500)	230	(33.3)
A71-702A-02	1093	(2000)	117	(17.0)
A71-702B-02	1093	(2000)	114	(16.5)
A71-718-01	1093	(2000)	111	(16.1)
A71-494C	1204	(2200)	39	(5.7)
A71-698B	1204	(2200)	46	(6.7)
A71-718-02	1204	(2200)	37	(5.4)

Loading rate = 0.025 cm/hr (0.01 in./min)
Shearing span distance = 0.025 cm (0.010 in.)
Diameter of bolt shank [0.635 cm (0.250 in.)] used in calculating shear area
Specimen head height = 0.32 cm (0.125 in.)

The longitudinal shear strength values were determined using the diameter of the bolt shank in calculating the shear area. This approximation was used because the actual sheared area, as seen in Fig. 19, was not perfectly cylindrical at the lower temperatures which reflects the effect of the different orientations of the lamellae in the various grains sheared. An example of this is shown in Fig. 20 where most of the shear failure occurred at grain boundaries with some interlamellar separation evident.

The effective longitudinal shear stress vs. displacement curves for the Ni_3Al-Ni_3Cb eutectic at the six temperatures tested are shown in Fig. 21. It is interesting to note that although the stress-displacement behavior of the samples tested at room temperature, 260°C (500°F) and 538°C (1000°F) is essentially elastic to failure, there is evidence of plasticity in the samples tested at 816°C (1500°F). The large amount of plasticity at the two higher temperatures is not only evident from the curves in Fig. 21, but also from the photographs of the specimens tested at these temperatures and shown in Fig. 19.

Similar test specimens of the aluminum-modified (Co,Cr,Al)-$(Cr,Co)_7C_3$ eutectic for measuring longitudinal shear strength, shear parallel to the direction of solidification, were also ground to shape and tested. These results are given in Table VII.

Table VII

Longitudinal Shear Strength of (Co,Cr,Al)-$(Cr,Co)_7C_3$ Eutectic Solidified at 10 cm/hr

Specimen Number	Temperature		Effective Shear Strength	
	°C	(°F)	$10^6 N/m^2$	(10^3 psi)
A71-774A	24	(75)	318	(46.1)
A72-004A	24	(75)	306	(44.3)
A72-004B	260	(500)	322	(46.7)
A71-771A	538	(1000)	297	(43.0)
A71-771B	816	(1500)	180	(26.1)
A71-774B	1093	(2000)	50	(7.3)
A71-774C	1204	(2200)	27	(4.0)
A72-004C	1204	(2200)	28	(4.1)

Loading rate = 0.025 cm/hr (0.01 in./min)
Shearing span distance = 0.025 cm (0.010 in.)
Diameter of bolt shank [0.635 cm (0.250 in.)] used in calculating shear area
Specimen head height = 0.32 cm (0.125 in.)

Although the failure mode of most of these specimens did not appear to be purely shear, the shear strength values given in Table VII were determined by using the bolt shank diameter, as noted, in calculating the shear area. The temperature dependence of longitudinal shear strength of the (Co,Cr,Al)-$(Co,Cr)_7C_3$ alloy is shown in Fig. 22. The photographs of fractured specimens at the various temperatures shown in Fig. 22 clearly indicate a transition from a tensile mode of failure to a shear mode of failure with increasing temperature.

The effective longitudinal shear stress vs. displacement curves for this fibrous eutectic are shown in Fig. 23. Again, as in the lamellar Ni_3Al-Ni_3Cb eutectic, the stress-displacement behavior is essentially elastic to failure for samples tested at 538°C (1000°F) and below, whereas there is evidence of increasing plasticity for samples tested at 816°C (1500°F) and above.

Longitudinal Thread Shear

Longitudinal thread shear specimens 5 cm (2 in.) long with 1/4-20 threads at either end were ground from both eutectic ingots with the direction of solidification parallel to the long dimension. Tables VIII and IX present the results of the longitudinal thread shear strength measurements using the test fixture shown in Fig. 6.

Table VIII

Longitudinal Thread Shear Strength of Ni_3Al-Ni_3Cb Eutectic Solidified at 2 cm/hr

Specimen Number	Temperature °C	Temperature (°F)	Approx. No. of Threads Engaged	Shear Strength $10^6 N/m^2$	Shear Strength (10^3 psi)	Failure
A71-337H-1	24	(75)	3	---	---	Tensile
A71-337H-2	24	(75)	3	---	---	Tensile
A71-337H-3	24	(75)	2	---	---	Tensile
A71-337H-4	24	(75)	1	250	(36.3)	Shear
A71-491-02	24	(75)	1	275	(39.8)	Shear
A71-491-03	24	(75)	1	199	(28.9)	Shear
A71-337H-4	121	(250)	2	286	(41.4)	Shear
A71-397-02A	121	(250)	2	325	(47.1)	Shear
A71-397-02B	260	(500)	2	343	(49.7)	Shear
A71-397-03A	260	(500)	2	382	(55.4)	Shear
A71-397-03B	371	(700)	2	386	(54.0)	Shear
A71-491-01	371	(700)	2	316	(45.8)	Shear
A71-491-01	371	(700)	3	---	---	Tensile

Loading rate = 0.025 cm/min (0.01 in./min)

Table IX

Longitudinal Thread Shear Strength of (Co,Cr,Al)-$(Cr,Co)_7C_3$ Eutectic Solidified at 10 cm/hr

Specimen Number	Temperature °C	Temperature (°F)	Approx. No. of Threads Engaged	Shear Strength $10^6 N/m^2$	Shear Strength (10^3 psi)	Failure
A71-771C-1	24	(75)	3	---	---	Tensile
A71-771C-2	24	(75)	2	---	---	Tensile
A71-771C-3	24	(75)	1	668	(96.8)	Shear
A71-771C-4	24	(75)	1 1/2	615	(89.2)	Shear
A72-004D-1	121	(250)	2	---	---	Tensile
A72-004D-2	121	(250)	1 1/2	---	---	Tensile
A72-004D-3	121	(250)	1	444	(64.3)	Shear
A72-009A	260	(500)	1	608	(88.2)	Shear
A72-009B	371	(700)	1	495	(71.8)	Shear
A72-009C	371	(700)	2	---	---	Tensile

Loading rate = 0.025 cm/min (0.01 in./min)

Because of the difficulty in determining the shear area in these test samples, several shadowgraphs were taken from different sides of the shear fracture surface and different areas were obtained. The shear strength values varied depending on the area used in the calculation and therefore an average value was used. In some more difficult cases, the values were calculated from shear areas determined from actual measurements (the width and length of thread sheared and the remaining sheared diameter).

The temperature dependence of longitudinal thread shear strength of the Ni_3Al-Ni_3Cb eutectic is shown in Fig. 24. Although the thread shear strength values obtained are higher than the values reported for the longitudinal shear strengths, the behavior of both appears similar with respect to the materials response to temperature. The higher apparent thread shear strength values may be due to the difficulty in accurately determining the sheared area. Some of these sheared areas are shown in the photograph of a fractured threaded specimen in Fig. 24.

Although an increase in longitudinal shear strength with an increase in temperature was previously evident (Fig. 19), it is more dramatic in the longitudinal thread shear strength (Fig. 24). As previously mentioned, this is partly due to the increase in the flow stress of the Ni_3Al phase with temperature. This longitudinal shear strength increase in the thread tests may also be due in part to the increasing shear ductility which would allow more uniform engagement of the specimen threads and test adapter.

The temperature dependence of longitudinal thread shear strength of the (Co,Cr,Al)-$(Cr,Co)_7C_3$ eutectic is also shown in Fig. 24. The thread shear strength values obtained are higher than the values reported for the longitudinal shear strengths, but again the behavior of both appears similar with respect to the materials response to temperature. The higher apparent thread shear strength values may again be due to the difficulty in accurately determining the sheared area (see photograph in Fig. 24).

Torsion

Solid rods of the Ni_3Al-Ni_3Cb eutectic with the long axis parallel to the growth direction, were fractured in torsion. These results are listed in Table X.

The following equations (Ref. 12) were used in determining the values shown in Table X for the two strain gaged specimens.

Shear stress at proportional limit*	$\tau_{PL} = Tr/J$	(1)
Shear strain at proportional limit*	$\gamma_{PL} = 2\varepsilon\ (2/G.F.)$	(2)
Shear modulus**	$G = Tr/J\gamma$	(3)
Shear stress at failure	$\tau_f = 3\ M_f/2\pi\ r^3$	(4)

*Proportional limit is defined as the point where the shear-stress and shear-strain curve first deviates from linearity.

**Shear modulus is determined from the slope of the linear portion of the shear-stress, shear-strain curve.

Table X

Torsional Strength of Ni_3Al-Ni_3Cb Eutectic Solidified at 2 cm/hr

Specimen Number	Temperature °C	(°F)	θ_{PL} deg.	τ_{PL} $10^6 N/m^2$	(10^3psi)	γ_{PL} %	G $10^9 N/m^2$	(10^6psi)	θ_f deg.	τ_f $10^6 N/m^2$	(10^3psi)	γ_f %
*A70-434-01	24	(75)	---	152	(22)	0.21	73	(10.6)	---	421	(61)	--
A71-749	24	(75)	6.9	290	(42)	0.76	--	---	113	497	(72)	12.3
*A70-434-02	204	(400)	---	186	(27)	0.29	63.5	(9.2)	~270	497	(72)	~15.2
A71-750	204	(400)	5.5	269	(39)	0.61	--	---	159	511	(74)	17.4
A71-751	538	(1000)	6.9	324	(47)	0.76	--	---	299	580	(84)	32.7
A72-176	538	(1000)	5.5	228	(33)	0.60	--	---	469	870	(126)	51.2
A72-339	871	(1600)	5.9	173	(25)	0.64	--	---	529	331	(48)	57.8
A72-341	871	(1600)	3.5	207	(30)	0.38	--	---	484	331	(48)	52.9
A72-238	1204	(2200)	4.8	28	(4)	0.53	--	---	1089	48	(7)	118.8
A72-338	1204	(2200)	1.7	28	(4)	0.19	--	---	889	110	(16)	97.0

strain measured by a time scale which was converted to an angle of twist measurement
gage length = 2.5 cm (1 in.)
rate of applied torque = .67 RPM

G ≡ shear modulus
τ_{PL}, τ_f ≡ shear stresses at proportional limit and at failure
γ_{PL}, γ_f ≡ shear strains at proportional limit and at failure
θ_{PL}, θ_f ≡ angle of twist at proportional limit and at failure
* ≡ strain measured by bonded strain gages oriented in the direction of the principal stress [gage length = 5 cm (2 in.)]

where $T \equiv$ torque
$r \equiv$ radius of gage section
$J \equiv$ polar moment of inertia ($\pi D^4/32$), $D \equiv$ diameter of gage section
$\varepsilon \equiv$ strain output measurement
G.F. $\equiv$ strain gage factor
$M_f \equiv$ torsional moment or torque at failure

Shear stress values given for specimens where strain was measured by a time scale which was then converted to an angle of twist measurement (θ) were determined using Eqs. (1) and (4) for the shear stress at the proportional limit and at failure respectively. The shear strain values for these specimens at the proportional limit and at failure were calculated using the following equation:

$$\gamma = r\theta/L \qquad (5)$$

where $r \equiv$ radius of gage section
$\theta \equiv$ angle of twist
$L \equiv$ length of gage section

There is an appreciable difference in both the shear stress and shear strain values at the proportional limit for specimens tested under the same conditions depending on the method used for measuring strain. This difference, however, is substantially reduced when these values are compared at the point of failure. The approximate shear strain value given in Table X for specimen number A70-434-02 was determined using Eq. (5) and a visual measurement of the angle of twist after failure.

The torque vs. angle of twist curves for the Ni_3Al-Ni_3Cb alloy are shown in Fig. 25. The three curves, room temperature, 204°C (400°F) and 538°C (1000°F), essentially vary only in the degree of twist at failure which increases with increasing temperature. For these temperatures, characteristic of cold working, the torque increased continuously with angle of twist up to a maximum where the specimen separated. Also, the specimen tested at 538°C (1000°F) experienced cracking, as noted in Fig. 25, well before final failure occurred. The initial cracking was recorded at an angle of twist of 67.1 degrees. Using Eqs. (4) and (5), the shear stress and shear strain at crack initiation were calculated to be 386 x 10^6 N/m^2 (56 x 10^3 psi) and 7.3 percent respectively. This was the only Ni_3Al-Ni_3Cb specimen tested that experienced this cracking phenomenon. The specimen may have been precracked, but in any case it indicates that this material can withstand the presence of the crack while maintaining its load carrying capability. For temperatures characteristic of hot working, (e.g. 1600 and 2200°F) the torque reached a peak and then gradually fell until the specimen fractured. For the 871°C (1600°F) curve shown, this peak occurred at an angle of twist of 467 degrees, a maximum shear stress of 352 x 10^6 N/m^2 (51 x 10^3 psi) and a shear strain of 51 percent. The peak for the 1204°C (2200°F) test occurred at an angle of twist of 559 degrees and a shear stress and shear strain of 124 x 10^6 N/m^2 (18 x 10^3 psi) and 61 percent respectively. The corresponding fractured specimens at room temperature (brittle fracture) and 1204°C (ductile failure) are also shown in Fig. 25.

Solid rods of the (Co,Cr,Al)-$(Cr,Co)_7C_3$ eutectic with the long axis parallel to the growth direction, were fractured in torsion. These results are given in Table XI.

Table XI

Torsional Strength of (Co,Cr,Al)-$(Cr,Co)_7C_3$ Eutectic Solidified at 10 cm/hr

Specimen Number	Temperature °C	(°F)	θ_{PL} deg.	τ_{PL} $10^6 N/m^2$	(10^3psi)	γ_{PL} %	G $10^9 N/m^2$	(10^6psi)	θ_f deg.	τ_f $10^6 N/m^2$	(10^3psi)	γ_f %
*A71-771D	24	(75)	---	228	(33)	0.27	83	(12.0)	---	---	--	--
A71-771D	24	(75)	6.9	386	(56)	0.76	--	---	126	614	(89)	13.8
*A71-771E	204	(400)	---	172	(25)	0.20	84	(12.2)	---	---	--	--
A71-771E	204	(400)	6.9	345	(50)	0.76	--	---	88	531	(77)	9.6
A71-774E	538	(1000)	3.5	248	(36)	0.38	--	---	253	552	(80)	27.6
A72-012A	538	(1000)	7.6	386	(56)	0.83	--	---	268	614	(89)	29.3
A72-004E	899	(1650)	2.1	62	(9)	0.23	--	---	349	69	(10)	38.1

strain measured by a time scale which was converted to an angle of twist measurement
gage length = 2.5 cm (1 in.)
rate of applied torque = .67 RPM

G ≡ shear modulus
τ_{PL}, τ_f ≡ shear stresses at proportional limit and at failure
γ_{PL}, γ_f ≡ shear strains at proportional limit and at failure
θ_{PL}, θ_f ≡ angle of twist at proportional limit and at failure
* ≡ strain measured by bonded strain gages oriented in the direction of the principal stress

The same equations described previously were used to determine the values listed in Table XI for this fibrous eutectic. The appreciable difference in shear stress and strain at the proportional limit for specimens tested under the same conditions but with different strain measuring methods is also present in these results.

The torque vs. angle of twist curves for the (Co,Cr,Al)-$(Cr,Co)_7C_3$ alloy are shown in Fig. 26. Again, as in the previous eutectic alloy study, the torque at temperatures up to and including 538°C (1000°F) increased with increasing angle of twist until it reached a maximum where the specimen failed. Only during the 899°C (1650°F) test did the torque increase to a peak and then decrease before the specimen fractured. This peak occurred at an angle of twist of 320 degrees, a maximum shear stress of 104×10^6 N/m^2 (15×10^3 psi) and a shear strain of 35 percent. Why the angle of twist at failure was less at 204°C (400°F) than at room temperature is not understood. Also, the specimen tested at 538°C (1000°F) experienced cracking, as noted in Fig. 26, well before final failure. The initial cracking was recorded at an angle of twist of 72.7 degrees. Using Eqs. (4) and (5), the shear stress and shear strain at crack initiation were calculated to be 483×10^6 N/m^2 (70×10^3 psi) and 7.9 percent respectively. This was the only (Co,Cr,Al)-$(Cr,Co)_7C_3$ torsion specimen tested that experienced this cracking phenomenon and, as previously mentioned under the discussion of the Ni_3Al-Ni_3Cb torsion results, also indicates that this fibrous eutectic material can withstand cracks by picking up the load again after deforming. The corresponding fractured specimens at room temperature (brittle fracture) and 899°C (ductile failure) are also shown in Fig. 26.

Fabricating Techniques

Grinding

All the test specimens for determining the material properties pertinent to fastener application of both eutectic alloys were successfully fabricated by grinding.

A typical flush head fastener shape of the Ni_3Al-Ni_3Cb eutectic that was fabricated by grinding is shown in Fig. 27. The direction of solidification is parallel to the long axis of the fastener. Various lamellar orientations, all parallel to the growth direction, are evident from the two microstructural views in Fig. 27. Several double flush headed specimens were ground to shape from Ni_3Al-Ni_3Cb ingots directionally solidified at 2 cm/hr for use in evaluating this process as a method for fabricating fasteners.

Casting

Two mold designs were used for the purpose of determining the feasibility of directly casting the Ni_3Al-Ni_3Cb eutectic into a typical flush head fastener shape. One design allowed directional solidification to proceed from the fastener shank to the flush head and the other allowed directional solidification from the flush head shape into the shank. Figure 28 shows two eutectic ingots that were successfully solidified at 2 cm/hr using both of these designs. The center photographs in Fig. 28 show the ingots after removal from the high purity alumina mold in which they were directionally cast. There appears to be no

indication of a metal-mold reaction. The outermost photographs show the cast fastener shapes after macro-etching their surfaces. It is evident from the grain alignment seen in these photographs that the solidification was directional.

A double flush headed specimen of the Ni_3Al-Ni_3Cb eutectic that was cast into shape at 2 cm/hr is shown in Fig. 29. The top photograph shows the ingot after removal from the high purity alumina mold in which it was directionally cast. Again, there appears to be no indication of a metal-mold reaction. Microstructural examination of the views shown in Fig. 29 indicates a relatively gradual transition of the eutectic grain alignment through the two flush headed shapes of the cast ingot.

A few single and double 100° flush headed specimens of the Ni_3Al-Ni_3Cb eutectic were directionally cast in order to evaluate this process as a method of fabricating fasteners.

Creep Forming

Bar samples [0.635 cm (0.250 in.) diameter by approximately 5 cm (2 in.) long] of both the Ni_3Al-Ni_3Cb and the (Co,Cr,Al)-$(Cr,Co)_7C_3$ eutectics were ground with the direction of solidification parallel to the long dimension. Several attempts were made to hot forge the ends of these samples with a 100° flush head die. The two major problems encountered were the lack of temperature control and the high strain rate which in some cases caused the material to shatter. A hot forging temperature of approximately 1204°C (2200°F) was selected but often the sample temperature fell well below this level and in other instances some melting of the sample was evident.

These initial experiments led to the belief that a creep forming process where temperature and strain rate can be better controlled, may prove worthwhile in producing a satisfactory flush head fastener shape. Several 100° flush head fastener shapes of both alloys were successfully creep formed (Figs. 30, 31, and 32). No distortion occurred, the materials completely filled the die, and there was no problem with die release as the difference in thermal expansion between the die material and the alloys being formed automatically provided adequate clearance on cooling. Metallographic examination indicated favorable phase distribution and flow in the flush head area of both alloys (Figs. 31 and 32). The cellular Ni_3Al-Ni_3Cb eutectic grown at 16 cm/hr (Fig. 30) and the fibrous (Co,Cr,Al)-$(Cr,Co)_7C_3$ eutectic (Fig. 32) solidified at 10 cm/hr were more easily creep formed into shape than the lamellar Ni_3Al-Ni_3Cb grown at 2 cm/hr (Fig. 31). Several specimens were fabricated to determine the shear strength of these eutectic materials when made into a typical fastener shape using the creep forming process.

Evaluation of Fabricated Fasteners

Room Temperature Shear Strength

The longitudinal thread shear results for both eutectics indicated that shearing of threads was not a major problem. This study revealed that with adequate thread engagement (more than two threads) failure would occur either by shear or tension at the fastener head or by tension through the root of the

thread. With this knowledge and because of the directional nature of these eutectic microstructures which are affected by the processing method, the shear strength evaluation of fabricated fasteners was centered around the determination of the effective shear strength of the fastener heads only.

The results of the room temperature shear strength evaluation of 100° flush head fastener shapes of the Ni_3Al-Ni_3Cb eutectic for the three fabrication techniques are listed in Table XII.

Table XII

Room Temperature Shear Strength Evaluation of 100° Flush Head Fastener Shape of Ni_3Al-Ni_3Cb Eutectic Solidified at 2 cm/hr

Specimen Number	Fabrication Technique	Specimen Configuration	Effective Shear Strength		Failure Mode
			$10^6 N/m^2$	(10^3 psi)	
A71-735A	ground	double headed	257	(37.2)	Shear & Tensile
A71-735B	ground	double headed	182	(26.4)	Shear & Tensile
A72-217	cast	double headed	166	(24.0)	Tensile
A72-237	cast	double headed	161	(23.4)	Shear & Tensile
A72-217a	cast	single headed	138	(20.0)	Shear & Tensile
A71-692	cast	single headed	215	(31.2)	Shear & Tensile
A71-694	cast	single headed	181	(26.3)	Shear & Tensile
A71-461-02	creep formed	single headed	103	(14.9)	Tensile (partly cellular microstructure)
A71-493-1	creep formed	single headed	218	(31.6)	Tensile (lamellar microstructure)
A71-548-1*	creep formed	single headed	99	(14.4)	Tensile (cellular microstructure)

*Solidified at 16 cm/hr

Most of the effective shear stress values listed in Table XII compare favorably with those previously shown for room temperature in Table VI with the following exceptions, the higher value of 257 x 10^6 N/m^2 (37.2 x 10^3 psi) for the double headed ground specimen and the lower values of 99 and 103 x 10^6 N/m^2 (14.4 and 14.9 x 10^3 psi) for the creep formed specimens. These low values can be explained by the fact that microstructural examination after testing revealed that the specimens contained a cellular microstructure near the fastener head. This breakdown in the lamellar microstructure could cause a weakening of the material in that area when exposed to 1204°C (2200°F) during the forming process.

A limited evaluation of the (Co,Cr,Al)-$(Cr,Co)_7C_3$ eutectic is given in Table XIII. These specimens were all creep formed and the first two tested yielded values that compare closely to the values given for room temperature in Table VII which were determined using ground specimens. The third test of a creep formed specimen resulted in a much higher effective shear stress than the previous two. These results are quite encouraging and indicate that a more concentrated study into the feasibility of a thermal mechanical working process as a fabricating technique for eutectic materials should be continued.

Table XIII

Room Temperature Shear Strength Evaluation of 100° Flush Head Fastener Shape of (Co,Cr,Al)-$(Cr,Co)_7C_3$ Eutectic Solidified at 10 cm/hr

Specimen Number	Fabrication Technique	Specimen Configuration	Effective Shear Strength		Failure Mode
			$10^6 N/m^2$	(10^3 psi)	
#1	creep formed	single headed	294	(42.6)	Tensile
#2	creep formed	single headed	316	(45.7)	Tensile
#3	creep formed	single headed	475	(68.8)	Tensile

Effect of Flush Head Angle on Room Temperature Shear Strength

Double flush-headed specimens of the Ni_3Al-Ni_3Cb eutectic which were ground to shape, were tested to determine the effective longitudinal shear strength (shear parallel to the direction of solidification) at room temperature of this material as a function of flush-head angle. The results are given in Table XIV.

Table XIV

Room Temperature Longitudinal Shear Strength of Ground Flush-Head Shapes of Ni_3Al-Ni_3Cb Eutectic Solidified at 2 cm/hr

Specimen Number	Flush Head Angle to Vertical	Effective Shear Strength	
	Degrees	$10^6 N/m^2$	(10^3 psi)
A71-742B	10	270	(39.1)
A71-748B	10	263	(38.1)
A71-742A	20	239	(34.6)
A71-748A	20	261	(37.8)
A72-441-01	45	177	(25.6)
A72-462-02	45	212	(30.7)
A71-735A	50	257	(37.2)
A71-735B	50	182	(26.4)

loading rate = 0.025 cm/hr (0.01 in./min)
diameter of bolt shank [0.635 cm (0.250 in.)] and height of fractured head used in calculating shear area.

The effect of flush head angle on the room temperature longitudinal shear strength of this alloy is shown in Fig. 33. The influence of higher compressive forces perpendicular to the tapered surface are evident by the increase in the effective shear strength with a decrease in flush head angle. The previously determined values, where the head was perpendicular ($\theta = 90°$) to the shank, are also shown in Fig. 33 along with photographs of fractured specimens illustrating the change in failure mode with the change in the head angle.

Effect on Room Temperature Torsional Strength after Exposure at 2200°F

The results of the room temperature torsional tests after exposure at 1204°C (2200°F) are shown in Table XV for the Ni_3Al-Ni_3Cb eutectic and in Table XVI for (Co,Cr,Al)-$(Cr,Co)_7C_3$. Little or no effect can be seen on the room temperature torsional strength after exposure at 1204°C (2200°F) in the Ni_3Al-Ni_3Cb eutectic whereas a slight effect is evident in the (Co,Cr,Al)-$(Cr,Co)_7C_3$ alloy.

Table XV

Effect on the Room Temperature Torsional Strength of Ni_3Al-Ni_3Cb Eutectic Solidified at 2 cm/hr after Exposure at 2200°F

Specimen Number	Exposure Time min	θ_{PL} deg.	τ_{PL} $10^6 N/m^2$	τ_{PL} (10^3psi)	γ_{PL} %	θ_f deg.	τ_f $10^6 N/m^2$	τ_f (10^3psi)	γ_f %
A71-749	0	6.9	290	(42)	0.76	113	496	(72)	12.3
A72-180	30	6.6	304	(44)	0.72	121	483	(70)	13.2
A72-336	60	6.6	269	(39)	0.72	131	538	(78)	14.3
A72-196	120	6.9	324	(47)	0.76	120	496	(72)	13.1

strain measured by a time scale which was converted to an angle of twist measurement
gage length = 2.5 cm (1 in.)
rate of applied torque = .67 RPM

τ_{PL}, τ_f ≡ shear stresses at proportional limit and at failure
γ_{PL}, γ_f ≡ shear strains at proportional limit and at failure
θ_{PL}, θ_f ≡ angle of twist at proportional limit and at failure

Table XVI

Effect on the Room Temperature Torsional Strength of (Co,Cr,Al)-$(Cr,Co)_7C_3$ Eutectic Solidified at 10 cm/hr after Exposure at 2200°F

Specimen Number	Exposure Time min	θ_{PL} deg.	τ_{PL} $10^6 N/m^2$	τ_{PL} (10^3psi)	γ_{PL} %	θ_f deg.	τ_f $10^6 N/m^2$	τ_f (10^3psi)	γ_f %
A71-771B	0	6.9	386	(56)	0.76	126	614	(89)	13.8
A72-009D	30	5.2	269	(39)	0.57	166	635	(92)	18.1
A72-009E	60	5.9	248	(36)	0.64	175	580	(84)	19.1
A72-004F	120	6.8	310	(45)	0.74	225	662	(96)	24.6

Refer to Table XV for footnotes

Shear Rupture

The data obtained from the short-term stress-rupture tests that were run for both eutectic alloys are shown in Table XVII.

Table XVII

Stress Rupture Data on Double Headed Longitudinal Shear Specimens

Material	Specimen Number	Temperature °C	Temperature (°F)	Stress $10^6 N/m^2$	Stress (10^3psi)	Rupture Life (hrs)
Ni_3Al-Ni_3Cb (2 cm/hr)	A71-271	816	(1500)	121	(17.5)	80 >141
	A72-117-02	816	(1500)	138	(20.0)	35.8
	A72-188-01	816	(1500)	138	(20.0)	94.6
	A72-117-01	1093	(2000)	52	(7.5)	3.0
	A72-175	1093	(2000)	41	(6.0)	10.4
	A72-188-02	1093	(2000)	35	(5.0)	32.6
	A72-337-01	1093	(2000)	28	(4.0)	>219.2*
	A72-337-02	1093	(2000)	31	(4.5)	76.9
(Co,Cr,Al)-$(Cr,Co)_7C_3$ (10 cm/hr)	A71-774D-01	816	(1500)	110	(16.0)	6.2
	A71-774D-02	1093	(2000)	14	(2.0)	>120*

*no failure

Only the shear-rupture results for the Ni_3Al-Ni_3Cb eutectic alloy tested at 1093°C (2000°F) are plotted in Fig. 34 and are compared with longitudinal-rupture data obtained for this eutectic from a previous study (Ref. 1) and with thread-rupture data for TD NiCr (Ref. 9).

CONCLUSIONS

The present program has revealed that both the lamellar Ni_3Al-Ni_3Cb and the fibrous (Co,Cr,Al)-$(Cr,Co)_7C_3$ directionally solidified eutectic alloys show promise as candidate materials for high temperature fastener applications. The material properties pertinent to fastener applications which were determined for both alloys are encouraging and although no torsion data were available for comparison, the transverse shear values obtained for both eutectic alloys (based on double shear testing) indicated equal or higher strengths than that reported for dispersion strengthened metals (e.g. TD NiCr) which were selected in a previous study for potential use as structural fasteners. The stress-rupture characteristics of the Ni_3Al-Ni_3Cb eutectic compare favorably with that of TD NiCr considering the difference in the testing mode used in obtaining the data. Finally, this study has indicated that a eutectic material can be successfully formed to shape by grinding, casting, and thermal-mechanical working (creep forming).

ALLOY RECOMMENDATION FOR FURTHER EVALUATION

Under a current program funded by NASA-Lewis Research Center, NAS3-15562, a high-strength, Ni_3Cb-reinforced eutectic has been identified which combines the advantages of superior creep strength with high solidification-rate processing capability, e.g. the alloy has been grown in a plane-front mode at 50 cm/hr, i.e. a factor of 5 times higher than the Ni_3Al-Ni_3Cb eutectic described herein. There are indications that this material is more easily machined and that it may also be formed into a shape more readily by some means of thermal-mechanical working. In addition, a preliminary evaluation of the room temperature longitudinal shear property of this alloy has shown that its strength is approximately twice that of Ni_3Al-Ni_3Cb and its failure is ductile. It has a high longitudinal tensile ductility at room temperature, should be relatively notch-insensitive, and therefore offers the possibility of being a superior fastener alloy.

ACKNOWLEDGEMENTS

These individuals are cited for their efforts in the following areas:

Solidification: M. Lacombe, R. Wicks;
Metallography: J. Hermann
Mechanical Testing: E. Ahlberg, J. McHugh, G. Pinto.

The author gratefully acknowledges Dr. E. R. Thompson and Dr. C. O. Hulse for their technical contributions to the accomplishment of the program goals, and Miss J. Hurlburt, Mrs. D. Gelinas, and Miss B. Dearborn for preparing the manuscript.

REFERENCES

1. Thompson, E. R. and F. D. George: Investigation of the Structure and Properties of the Ni_3Al-Ni_3Cb Eutectic Alloy. Final Report, Contract N00019-69-C-0162 (July 31, 1969).

2. Thompson, E. R. and F. D. Lemkey: Structure and Properties of $Ni_3Al(\gamma')$-Based Eutectic Alloys. ASM Trans. Quarterly, Vol. 62, pp 140-154 (1969).

3. Thompson, E. R. and F. D. George: Eutectic Superalloys. 1969 SAE Transactions, Vol. 78, p 2283 (Dec. 1970).

4. Thompson, E. R., F. D. George, and E. H. Kraft: Investigation to Develop a High Strength Eutectic Alloy with Controlled Microstructure. Final Report, Contract N00019-70-C-0052 (July 31, 1970).

5. Thompson, E. R., E. H. Kraft, and F. D. George: Investigation to Develop a High Strength Eutectic for Aircraft Engine Use. Final Report, Contract N00019-71-C-0096 (July 31, 1971).

6. Thompson, E. R. and F. D. Lemkey: Unidirectional Solidification of Cobalt-Chromium-Carbon Monovariant Eutectic Alloys. Met. Trans., Vol. 1, p 2799 (1970).

7. Thompson, E. R., D. A. Koss, and J. C. Chesnutt: Mechanical Behavior of a Carbide Reinforced Cobalt-Chromium Eutectic Alloy. Met. Trans., Vol. 1, p 2807 (1970).

8. Thompson, E. R.: Anisotropic Toughness of a Carbide Reinforced Cobalt, Chromium Eutectic. J. Composite Mat., Vol. 5, p 235 (1971).

9. Roach, T. A.: Dispersion Strengthened Metals Structural Mechanical Fastener Evaluation. Tech. Report AFFDL-TR-68-89 (June 1968).

10. Metals Handbook, (American Society for Metals, Metals Park, Ohio, 1961), Eighth edition, Vol. 1, p 946.

11. Thornton, P. H., R. G. Davies, and T. L. Johnston: The Temperature Dependence of the Flow Stress of the γ' Phase Based Upon Ni_3Al. Met. Trans., Vol. 1, p 207 (1970).

12. Dieter, Jr., G. E.: Mechanical Metallurgy (McGraw-Hill Book Company, Inc., New York, 1961) pp 273-281.

L911174-11

MICROSTRUCTURES OF UNIDIRECTIONALLY SOLIDIFIED Ni_3Al–Ni_3Cb AND (Co,Cr,Al)–$(Cr,Co)_7C_3$ EUTECTICS

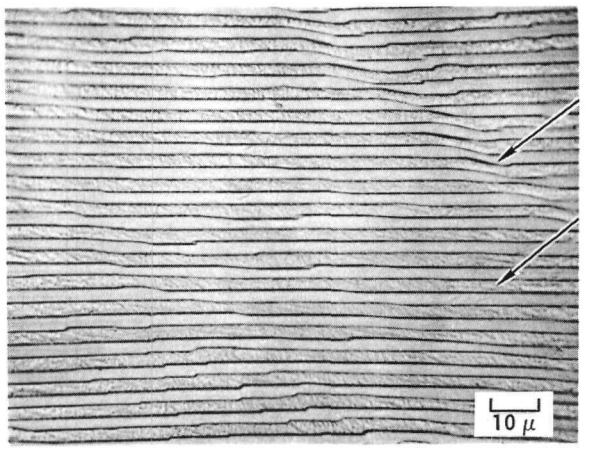

LONGITUDINAL

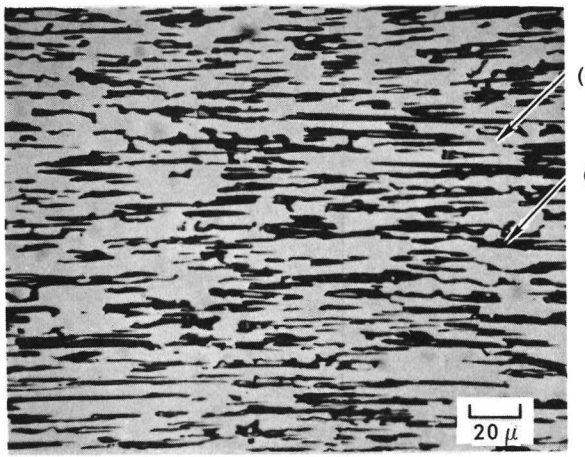

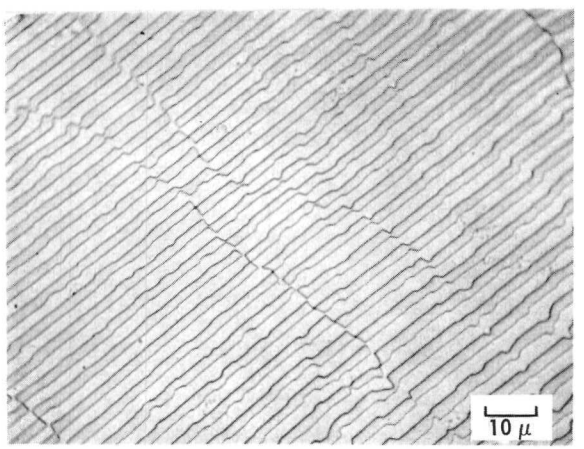

TRANSVERSE

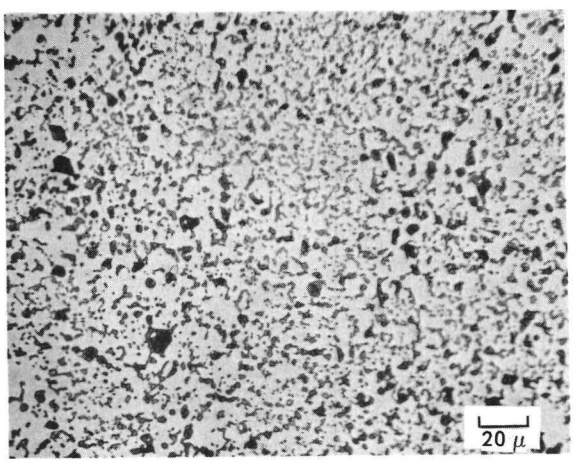

FIG. 1

FIG. 2

GRAPHITE DIRECTIONAL SOLIDIFICATION FURNACE

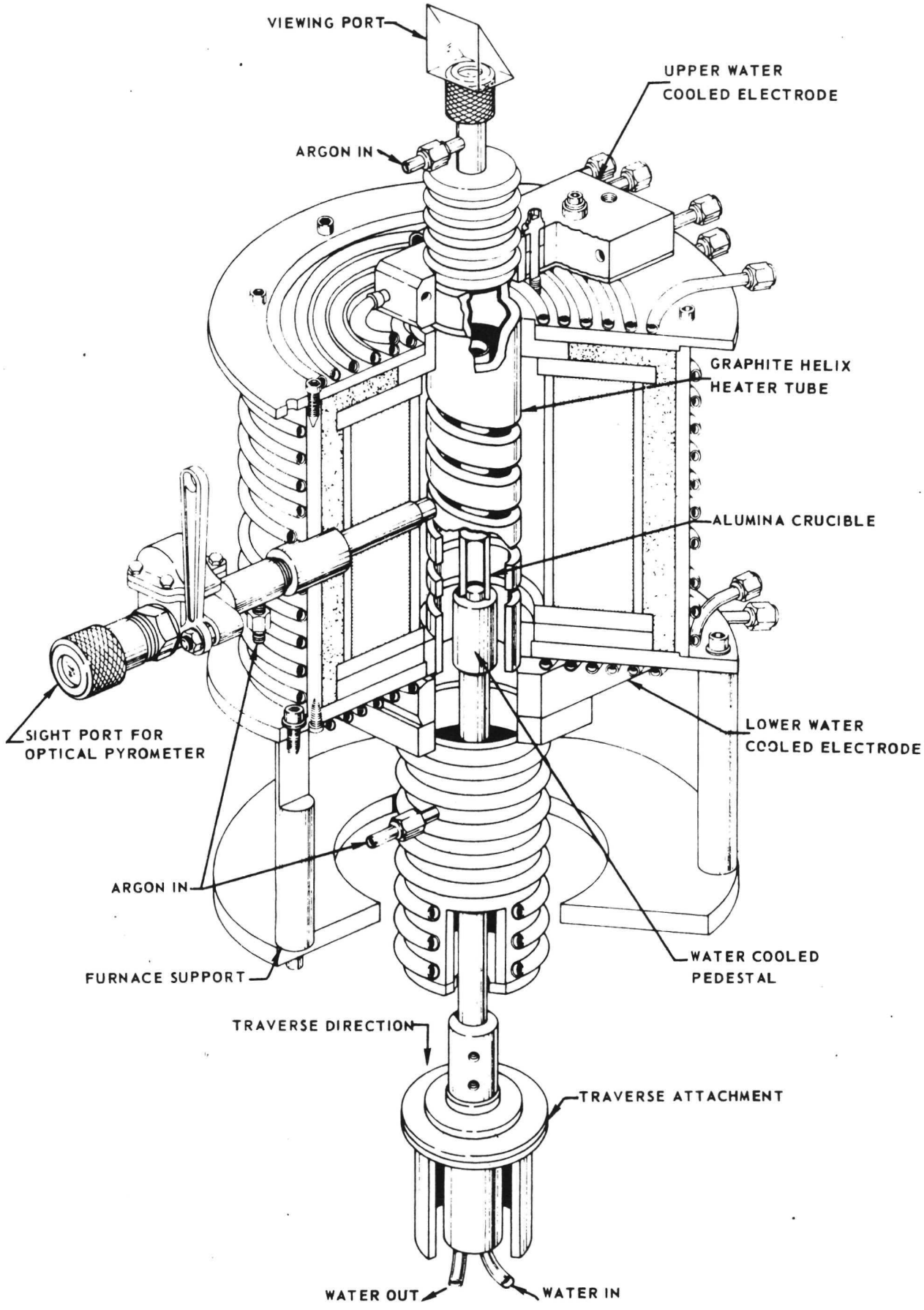

ROOM TEMPERATURE TRANSVERSE SHEAR FIXTURE WITH HARDENED STEEL LOADING FACES

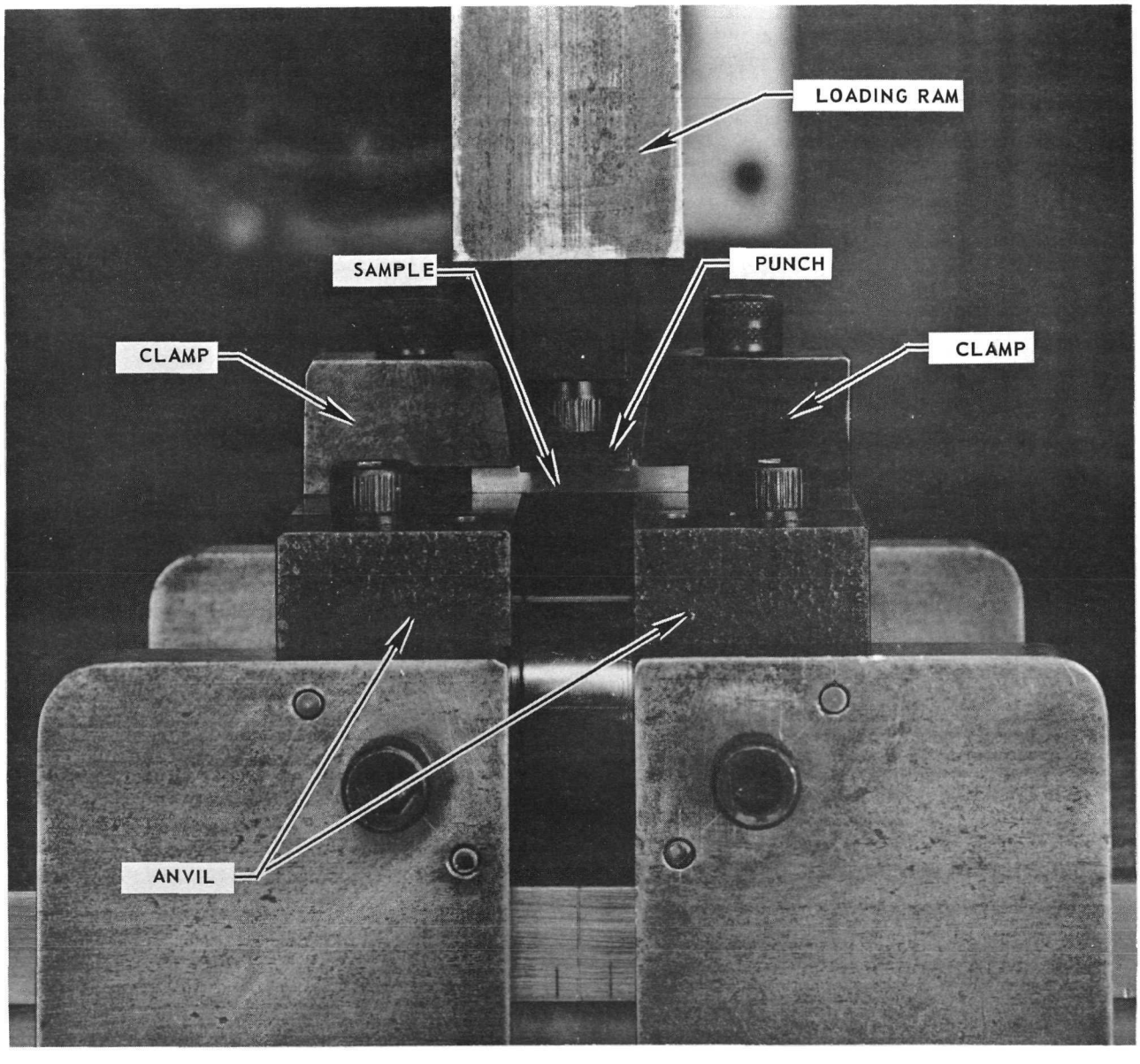

HIGH TEMPERATURE ALUMINA TRANSVERSE SHEAR FIXTURE

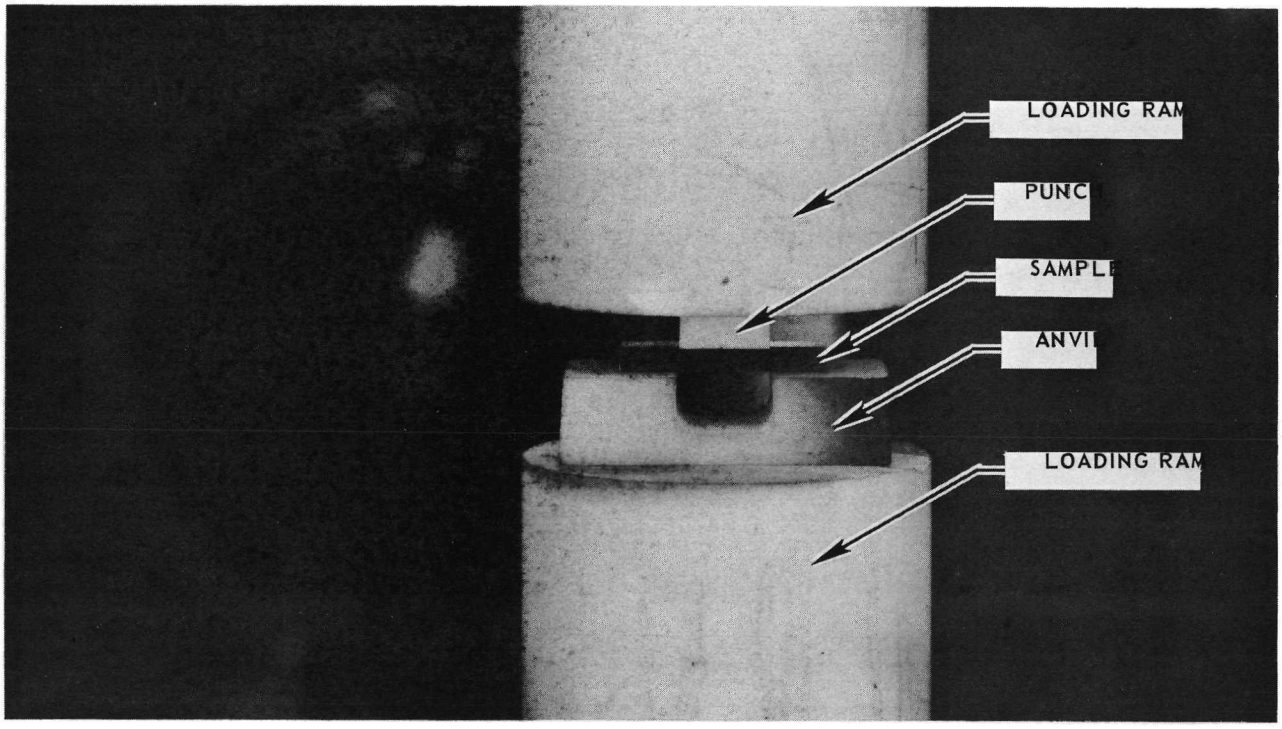

FIG. 5

LONGITUDINAL SHEAR FIXTURE

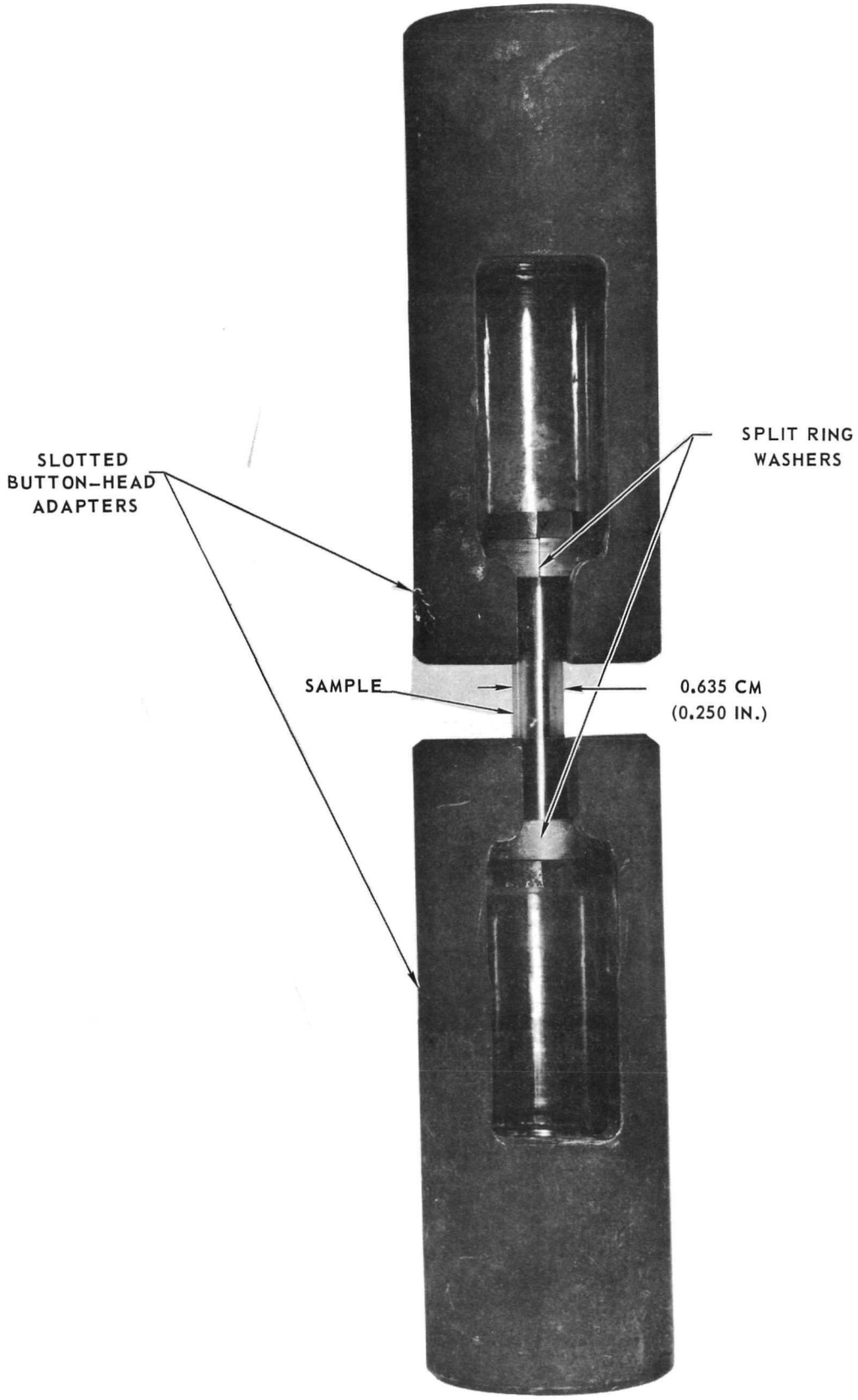

FIG. 6

THREAD SHEAR TEST FIXTURE

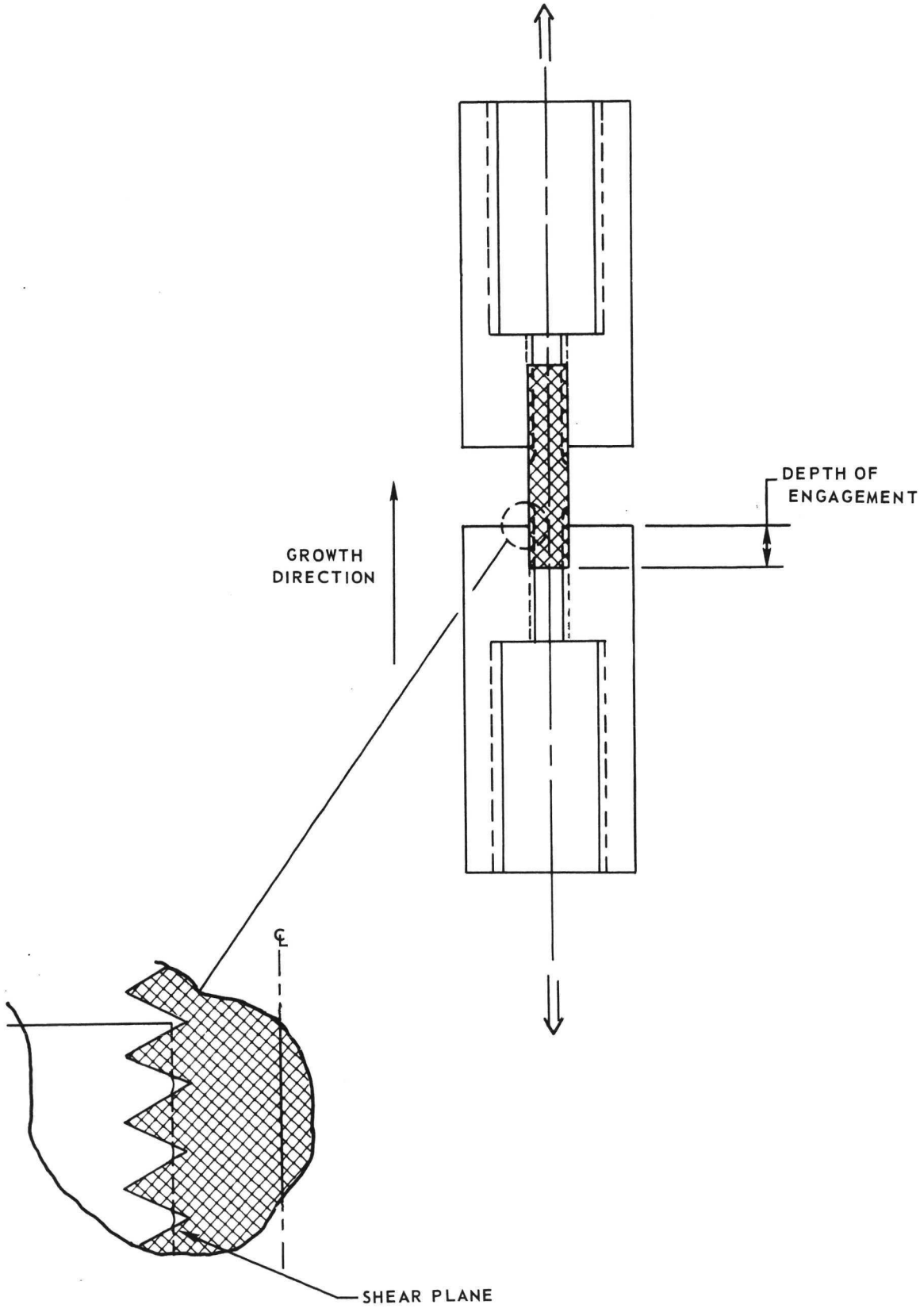

FIG. 7

LOW TEMPERATURE SOLID ROD TORSION TESTING APPARATUS

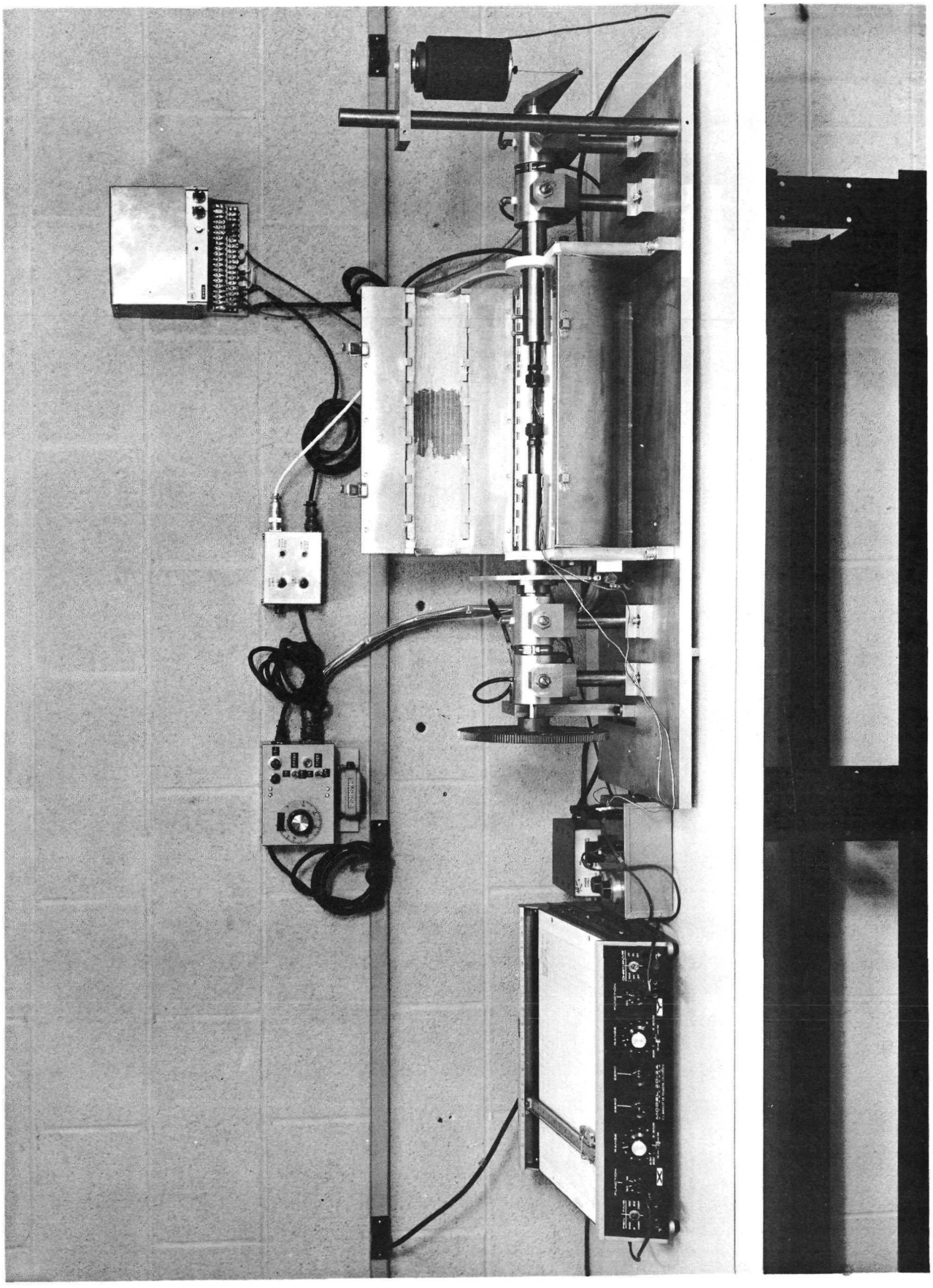

RL-70-97-D

FIG. 8

HIGH TEMPERATURE SOLID ROD TORSION TESTER

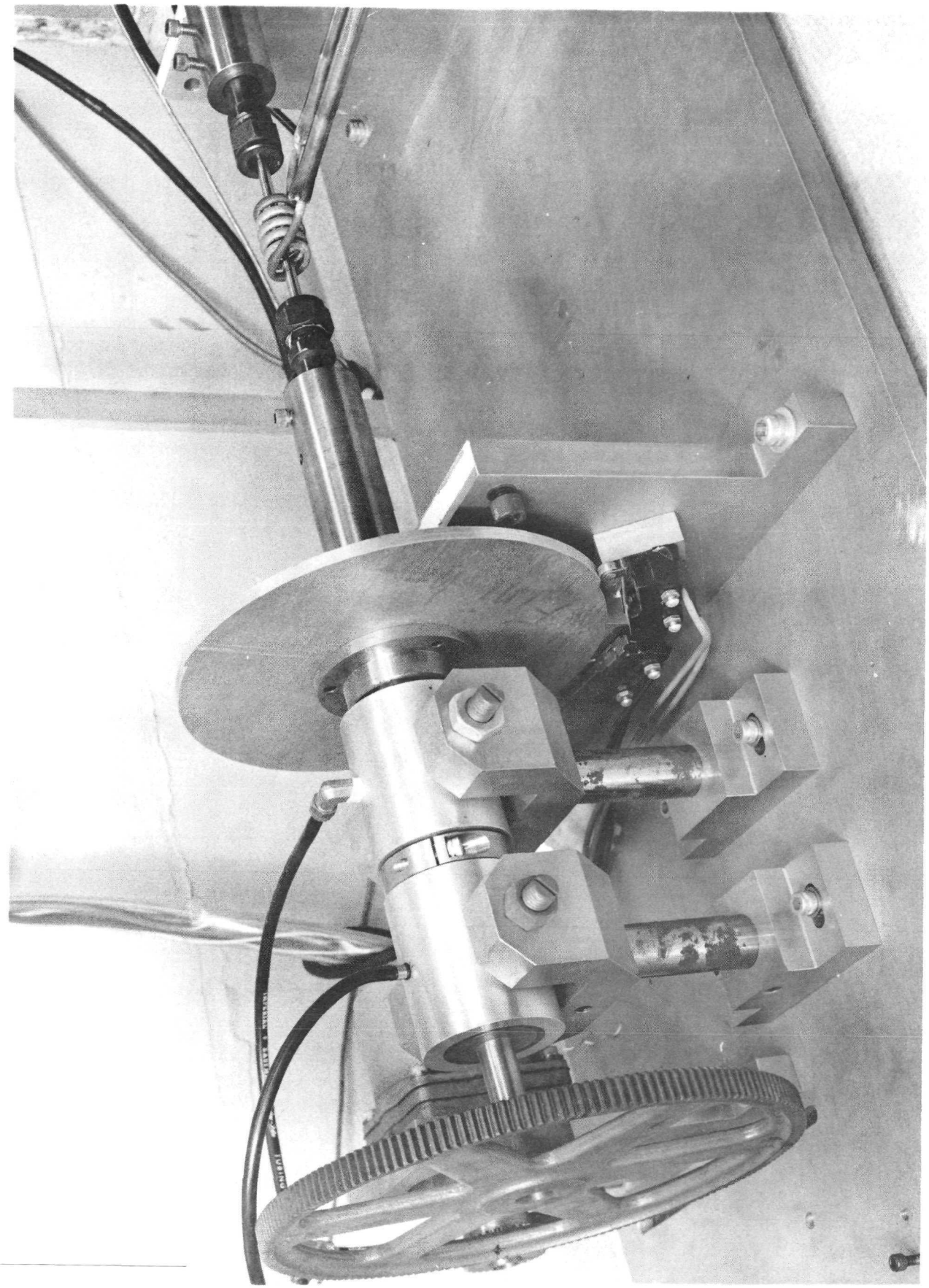

LONGITUDINAL SINGLE FLUSH HEAD TEST FIXTURE

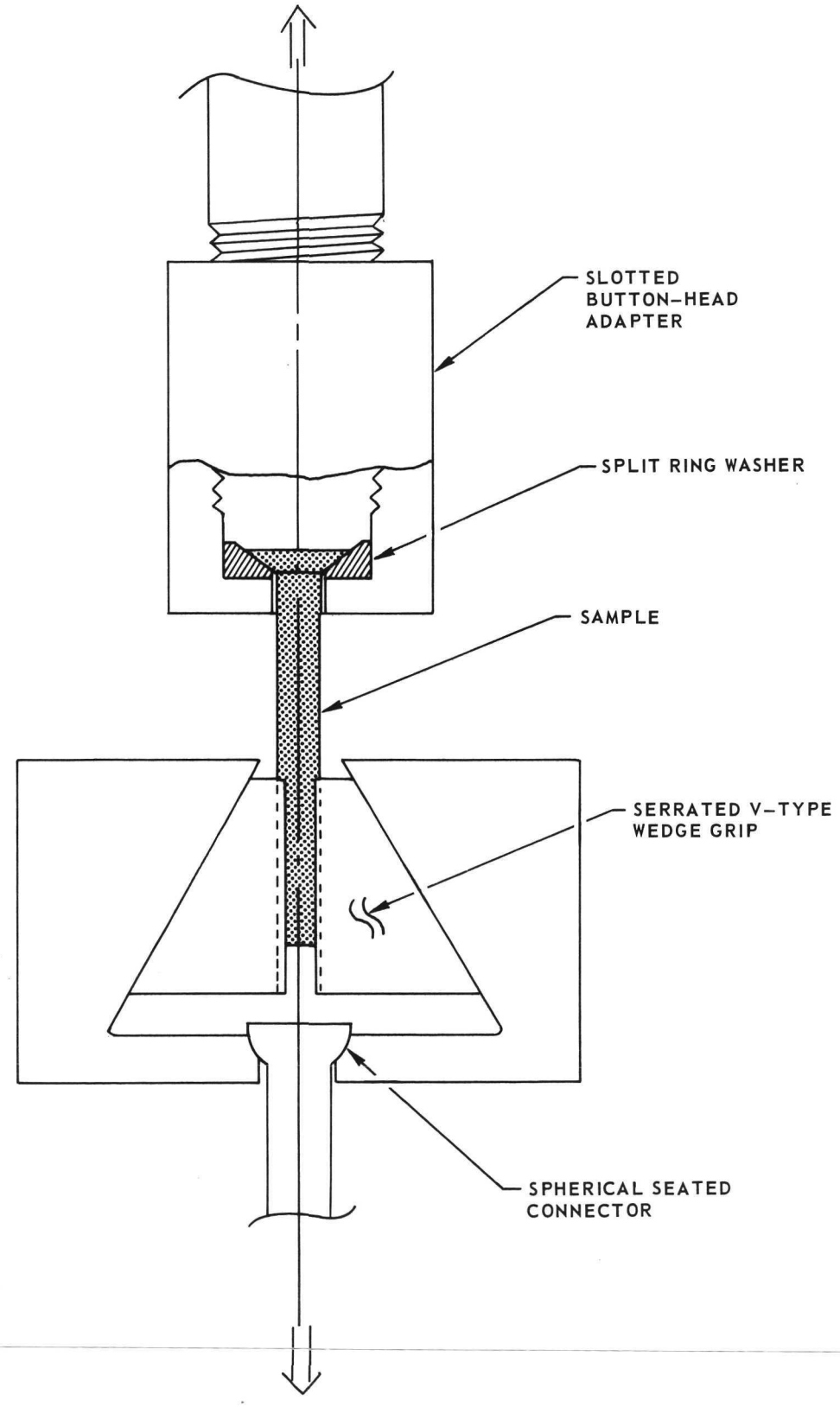

ROOM TEMPERATURE TRANSVERSE SHEAR STRENGTH VS SHEAR SPAN OF Ni_3Al–Ni_3 Cb EUTECTIC SOLIDIFIED AT 2 CM/HR

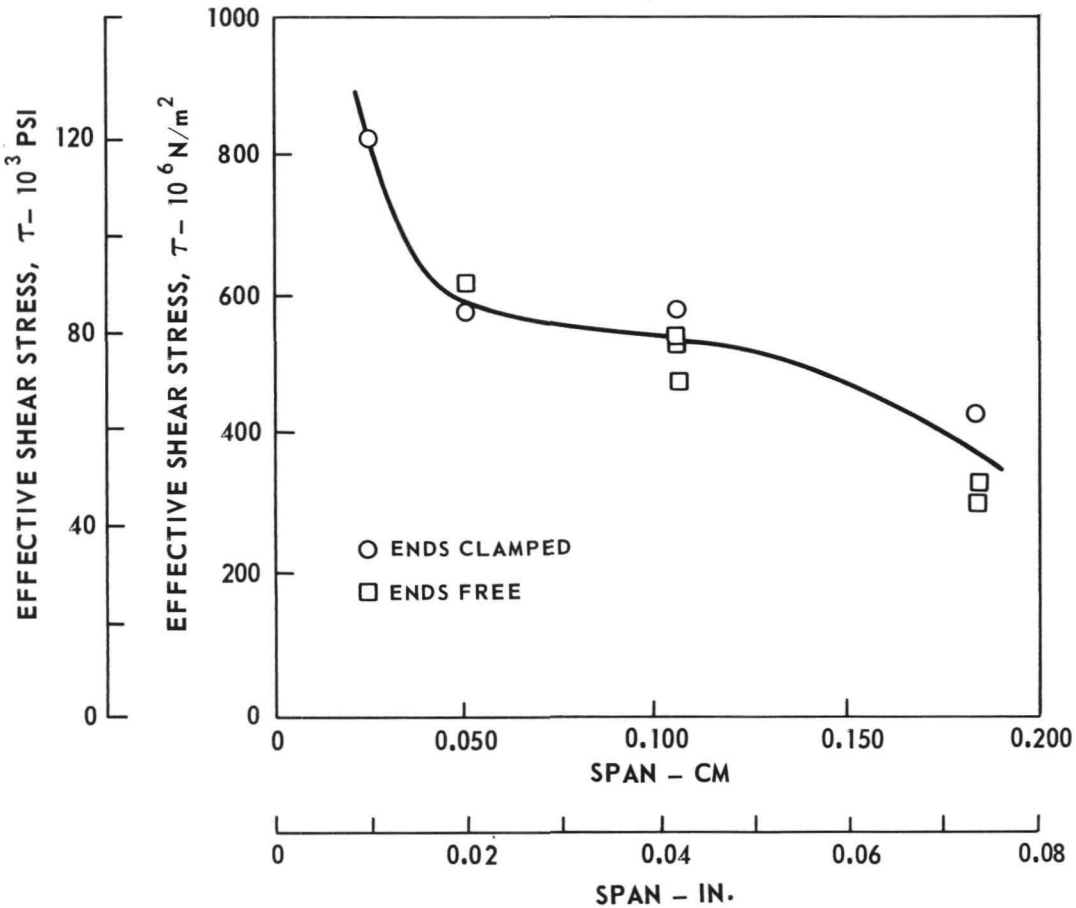

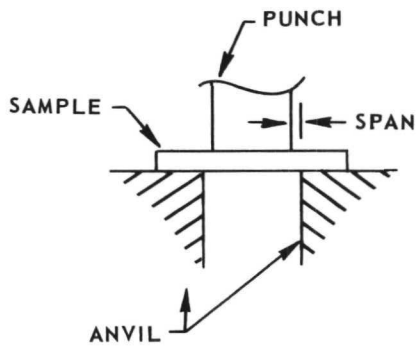

FIG. 10

TRANSVERSE SHEAR STRESS VS DEFLECTION FOR Ni_3Al–Ni_3Cb EUTECTIC SOLIDIFIED AT 2 CM/HR

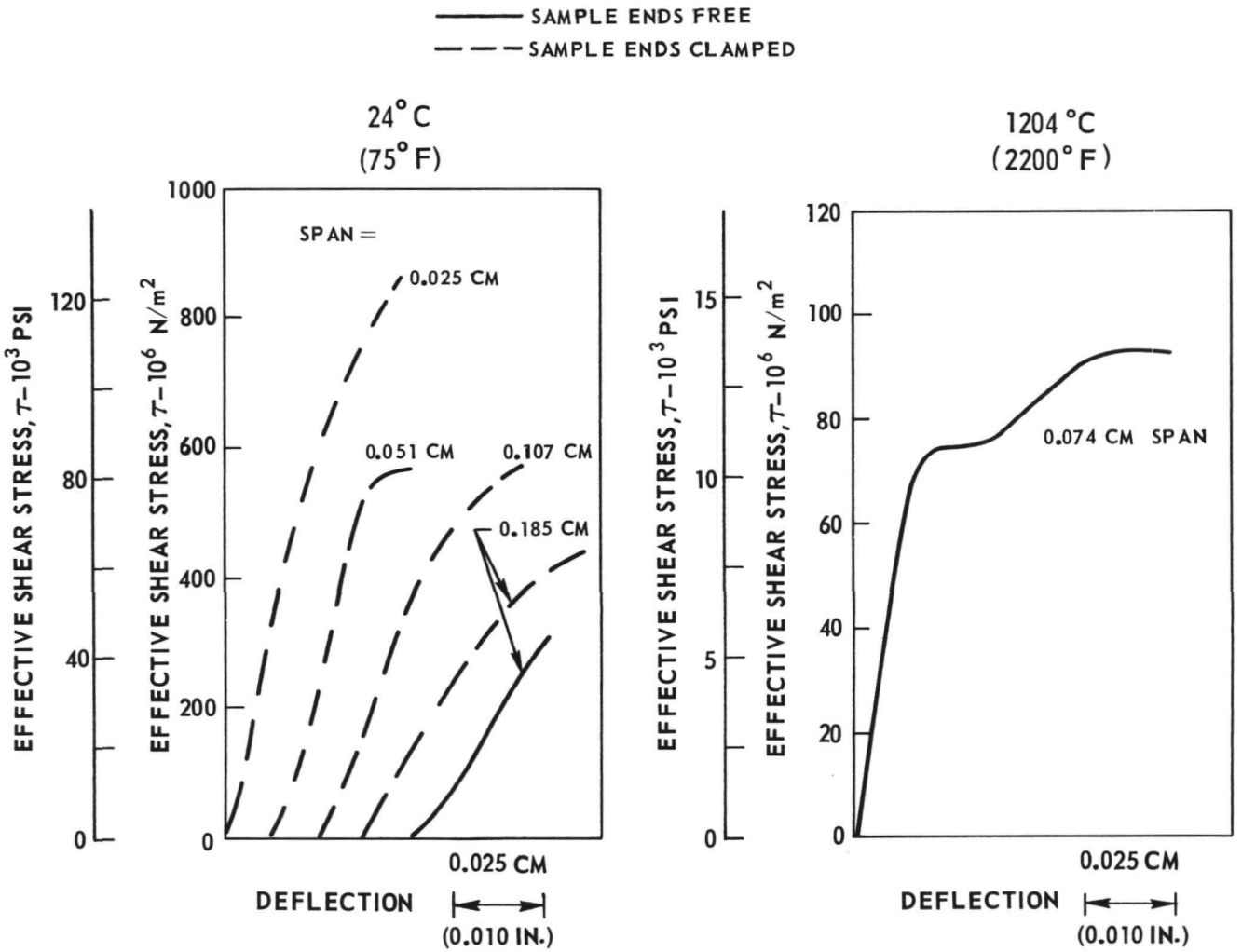

TEMPERATURE DEPENDENCE OF TRANSVERSE SHEAR STRENGTH OF Ni_3Al–Ni_3Cb EUTECTIC SOLIDIFIED AT 2 CM/HR

○ SAMPLE ENDS FREE AND CLAMPED; SPAN, 0.051 – 0.107 CM (0.020 – 0.042 IN.)

□ SAMPLE ENDS FREE; SPAN, 0.074 – 0.076 CM (0.029 – 0.030 IN.)

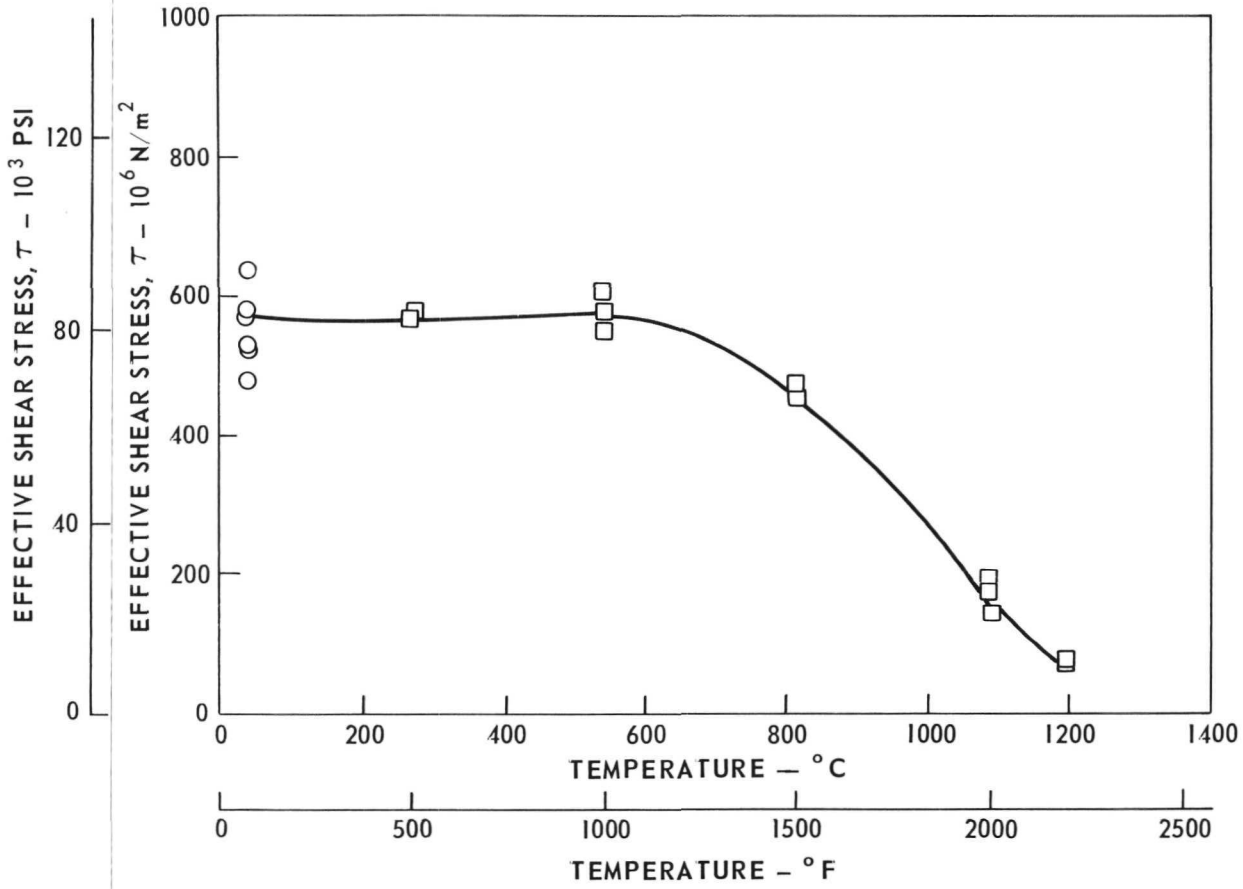

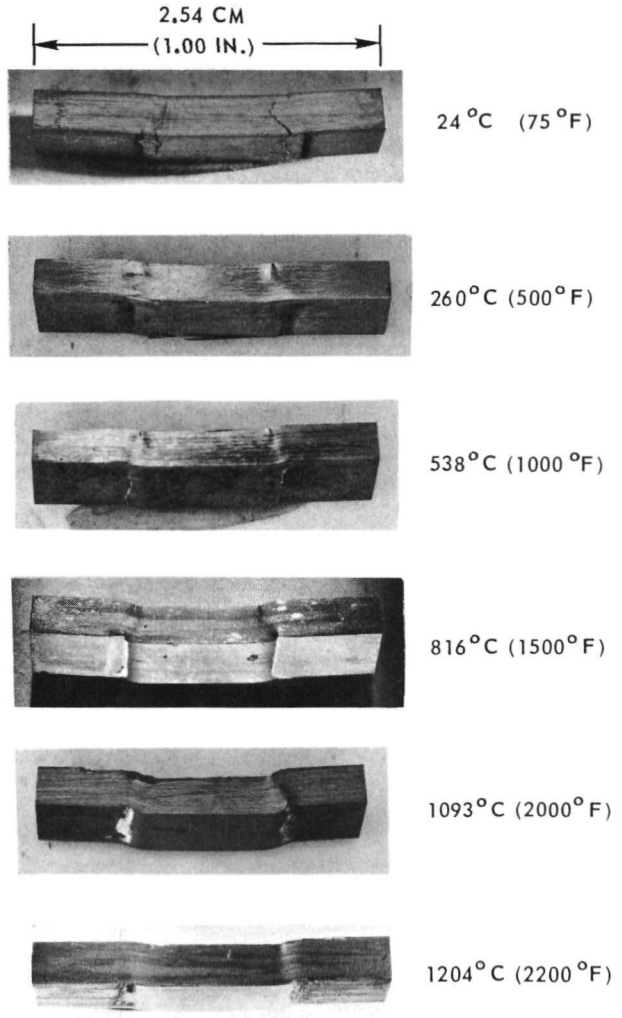

FIG. 12

L911174-11

ROOM TEMPERATURE TRANSVERSE SHEAR STRENGTH VS SHEAR SPAN OF (Co, Cr, Al) – $(Cr, Co)_7 C_3$ EUTECTIC SOLIDIFIED AT 10 CM/HR

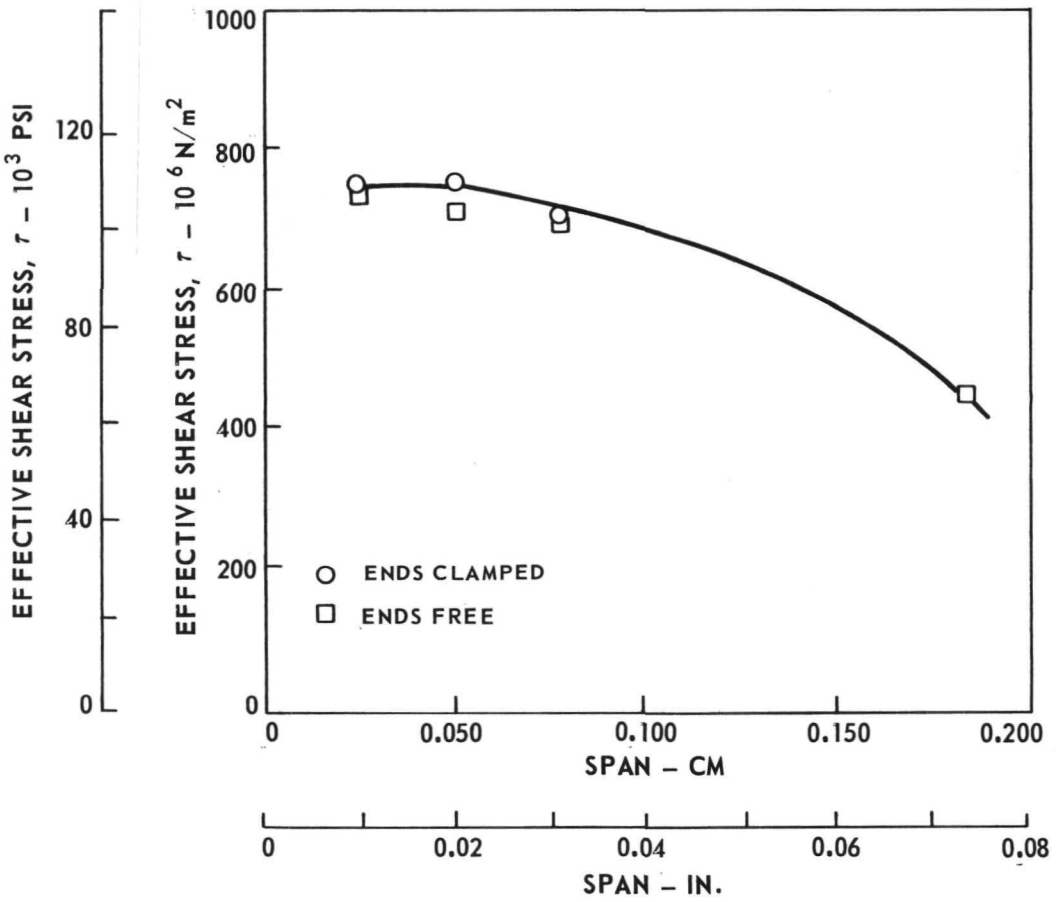

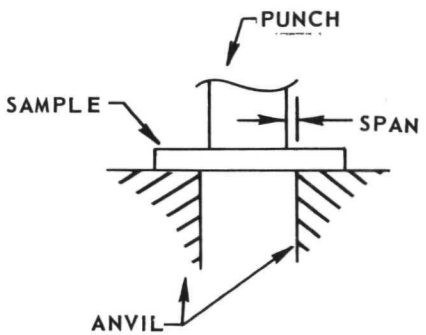

FIG. 13

TRANSVERSE SHEAR STRESS VS DEFLECTION FOR (Co, Cr, Al) – $(Cr, Co)_7C_3$ EUTECTIC SOLIDIFIED AT 10 CM/HR

SAMPLE ENDS FREE

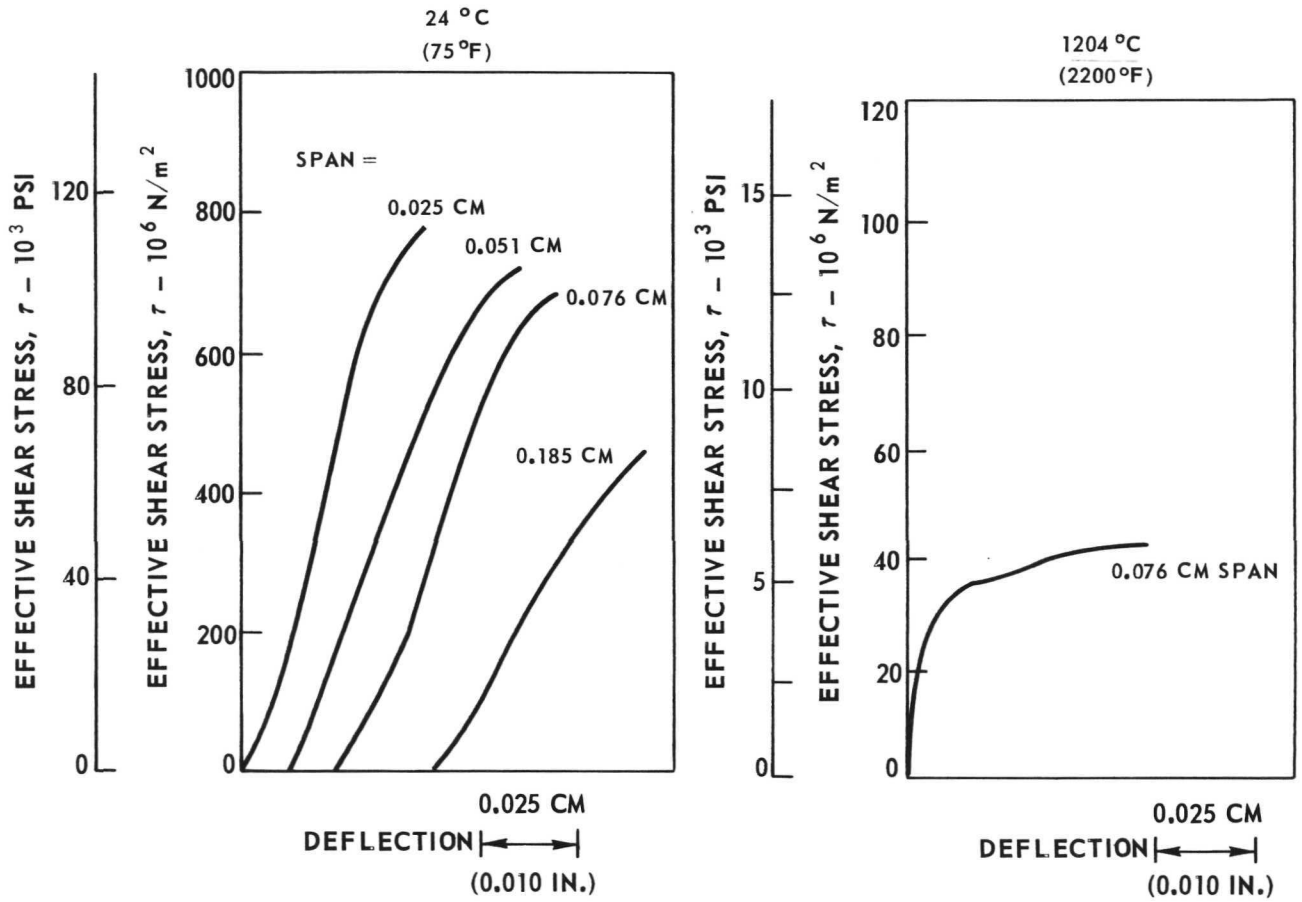

TEMPERATURE DEPENDENCE OF TRANSVERSE SHEAR STRENGTH OF (Co,Cr,Al)–$(Cr,Co)_7C_3$ EUTECTIC SOLIDIFIED AT 10 cm/hr

SAMPLE ENDS FREE (EXCEPT AS INDICATED); SPAN, 0.076 CM (0.030 IN.)

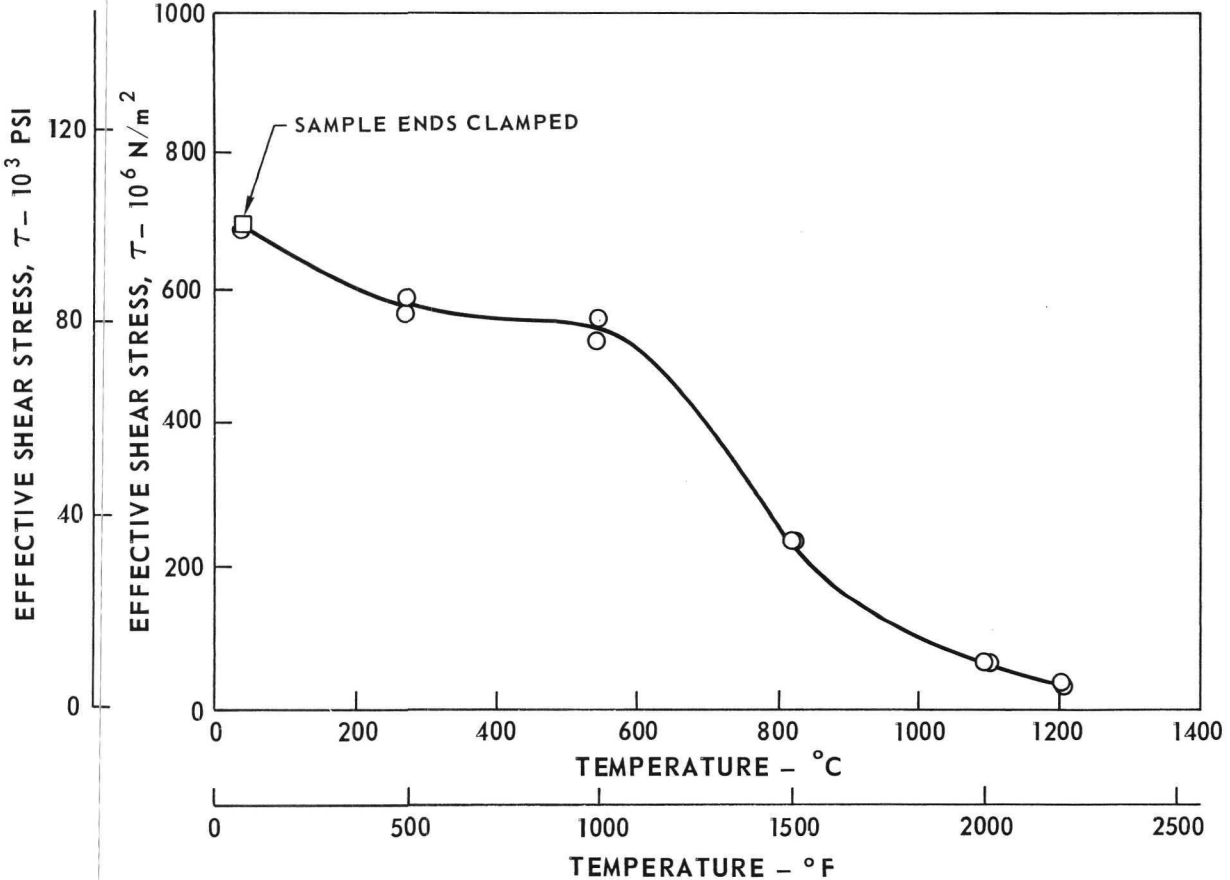

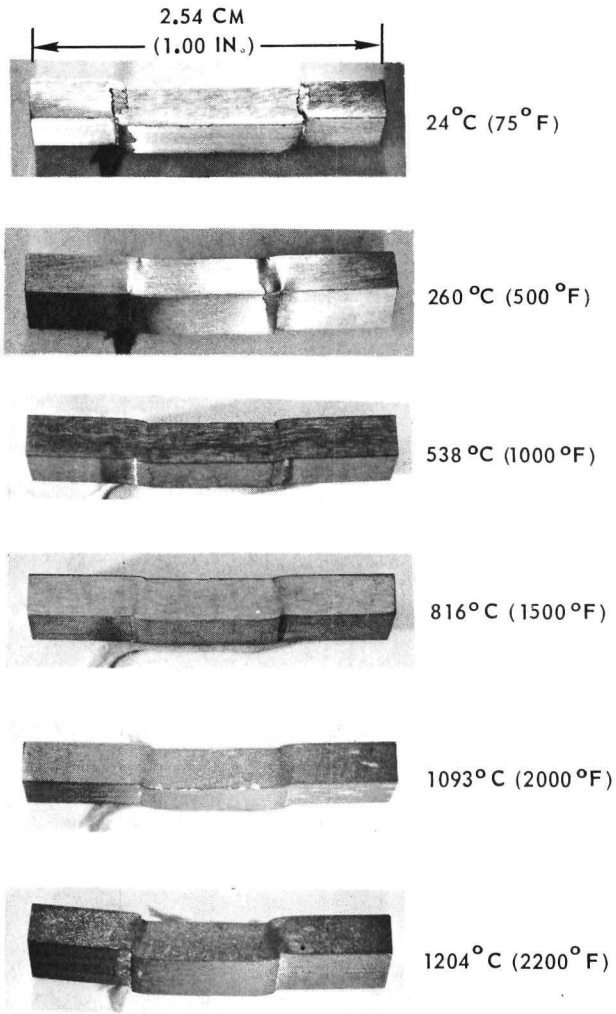

FIG. 15

L911174-11

FIG. 16

TEMPERATURE DEPENDENCE OF TRANSVERSE SHEAR STRENGTH

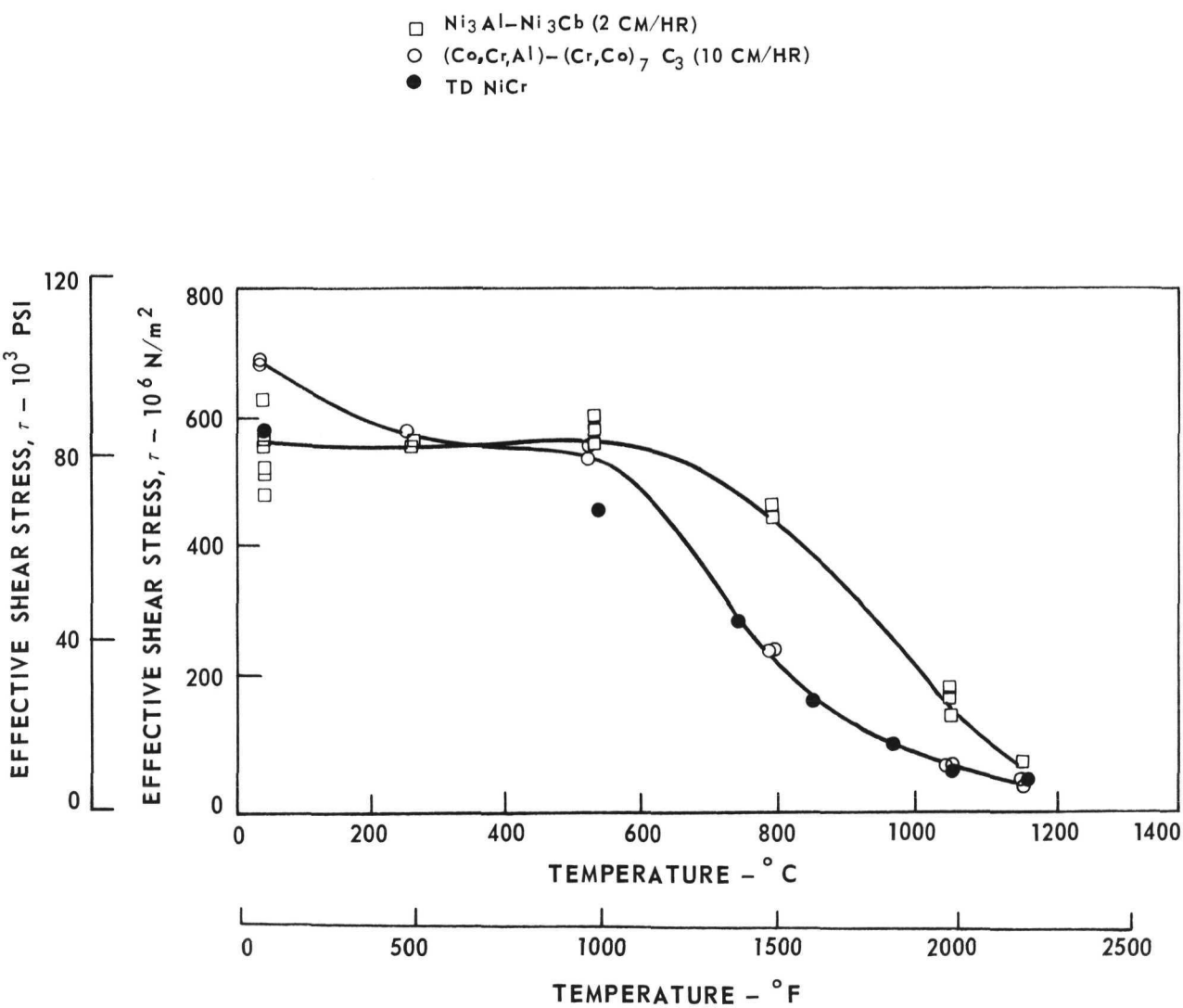

FIG. 17

ROOM TEMPERATURE FRACTURE MODES OF LONGITUDINAL SHEAR SPECIMENS

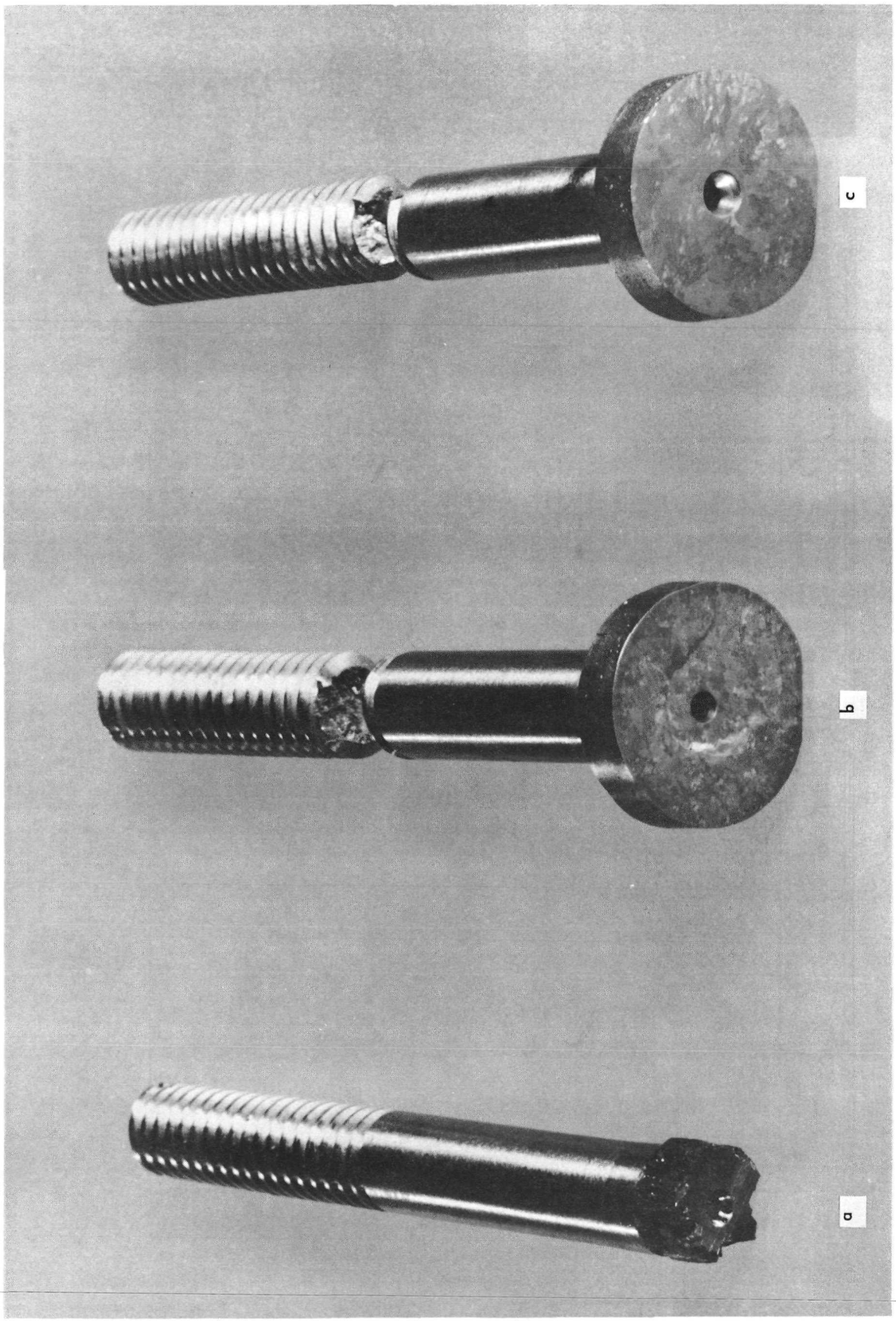

6061-T6 SHEAR SPECIMENS TESTED AT ROOM TEMPERATURE

#1

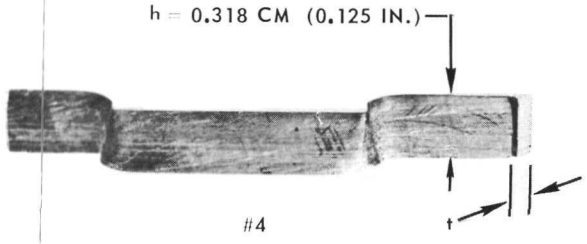

#4

SHEAR AREA = ht

t(CONSTANT) = 0.635 CM
(0.250 IN.)

#5

#8

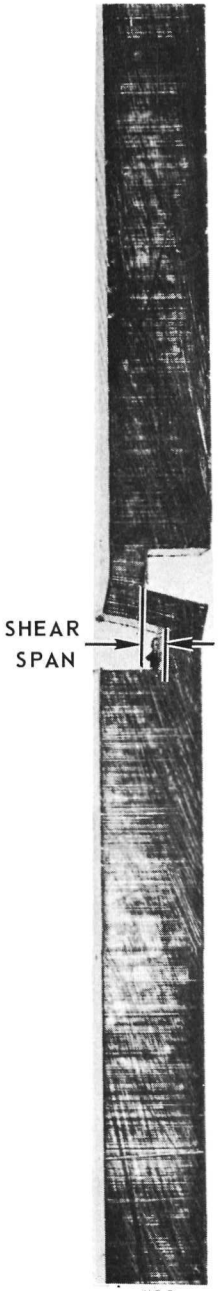

#11

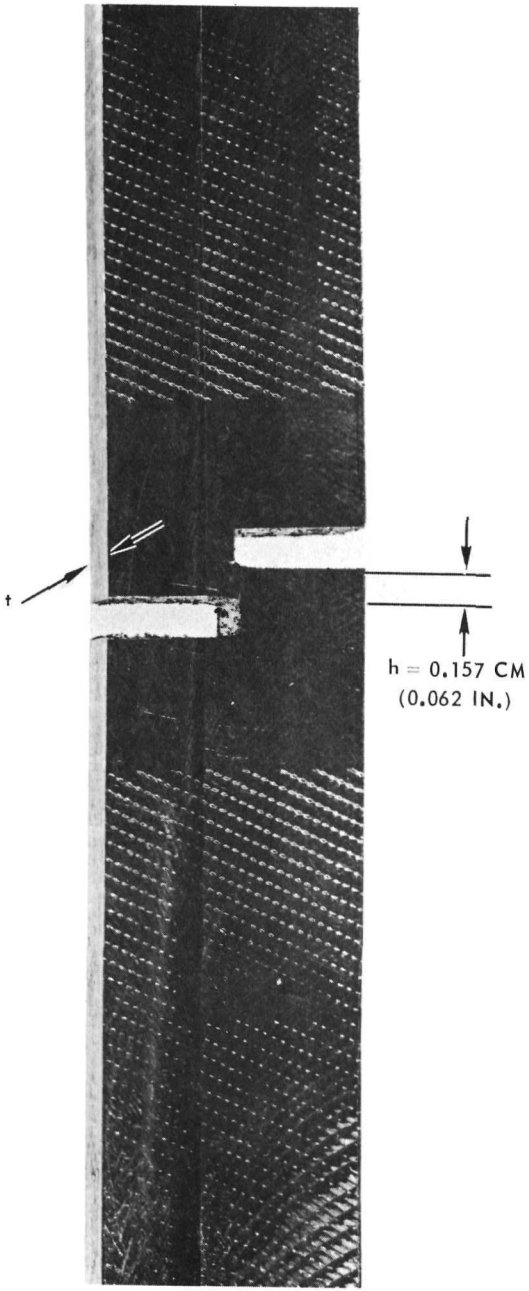

#16

FIG. 18

TEMPERATURE DEPENDENCE OF LONGITUDINAL SHEAR STRENGTH OF Ni_3Al–Ni_3Cb EUTECTIC SOLIDIFIED AT 2 CM/HR

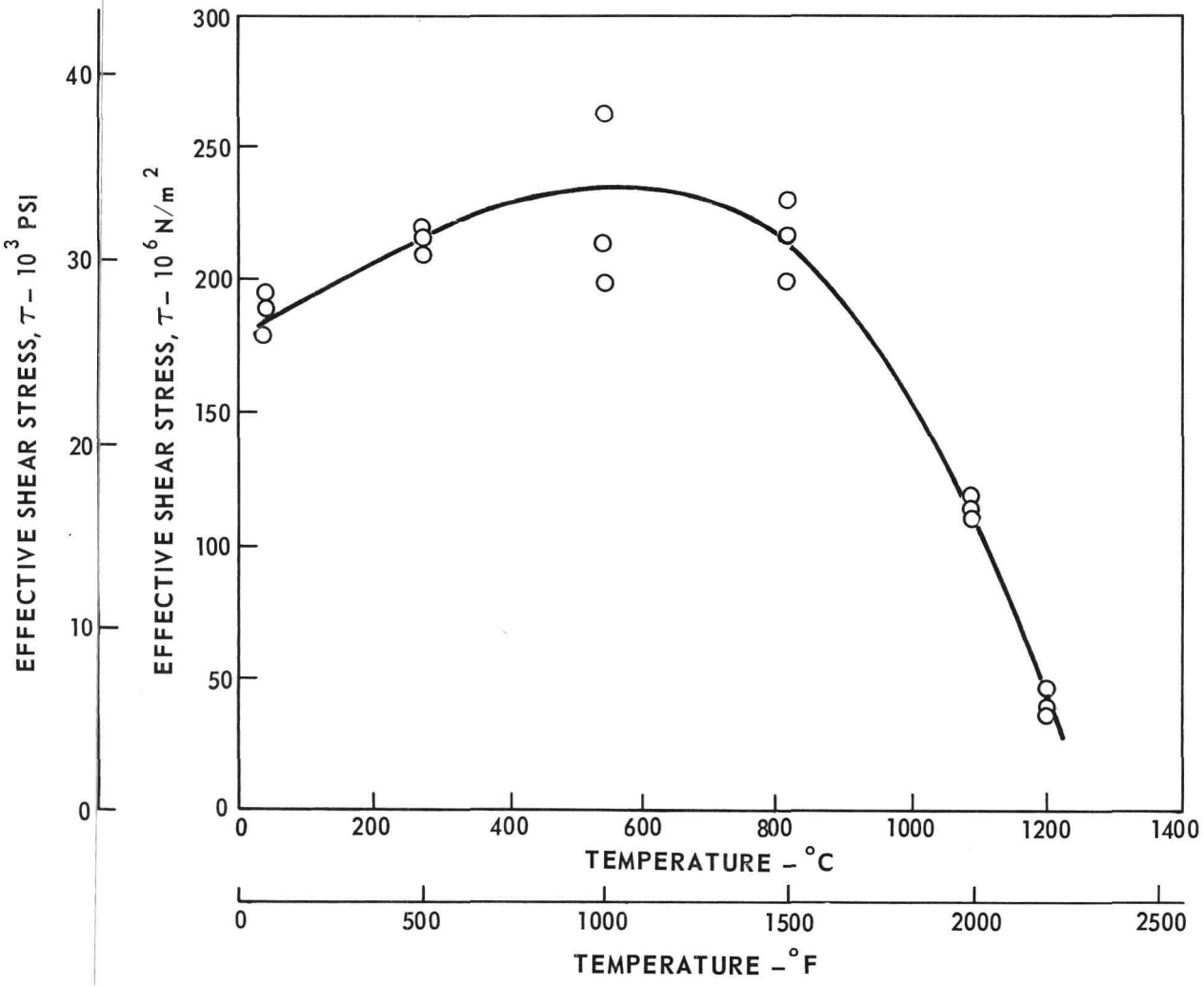

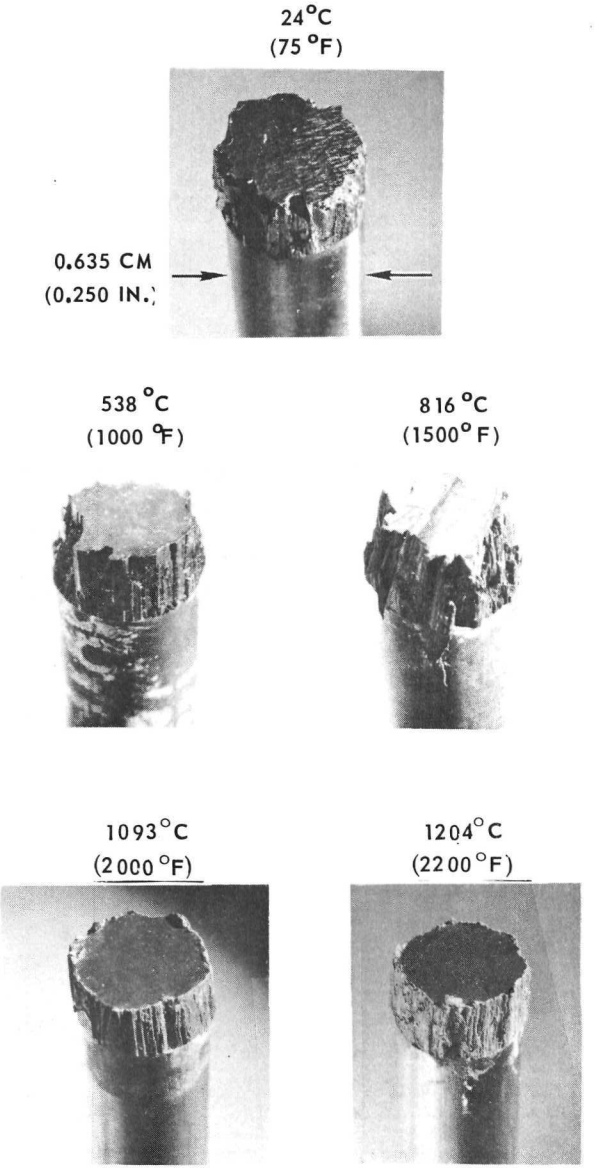

L911174-11

FIG. 19

FIG. 20

ROOM TEMPERATURE LONGITUDINAL SHEAR FAILURE OF Ni_3Al-Ni_3Cb EUTECTIC SOLIDIFIED AT 2 CM/HR

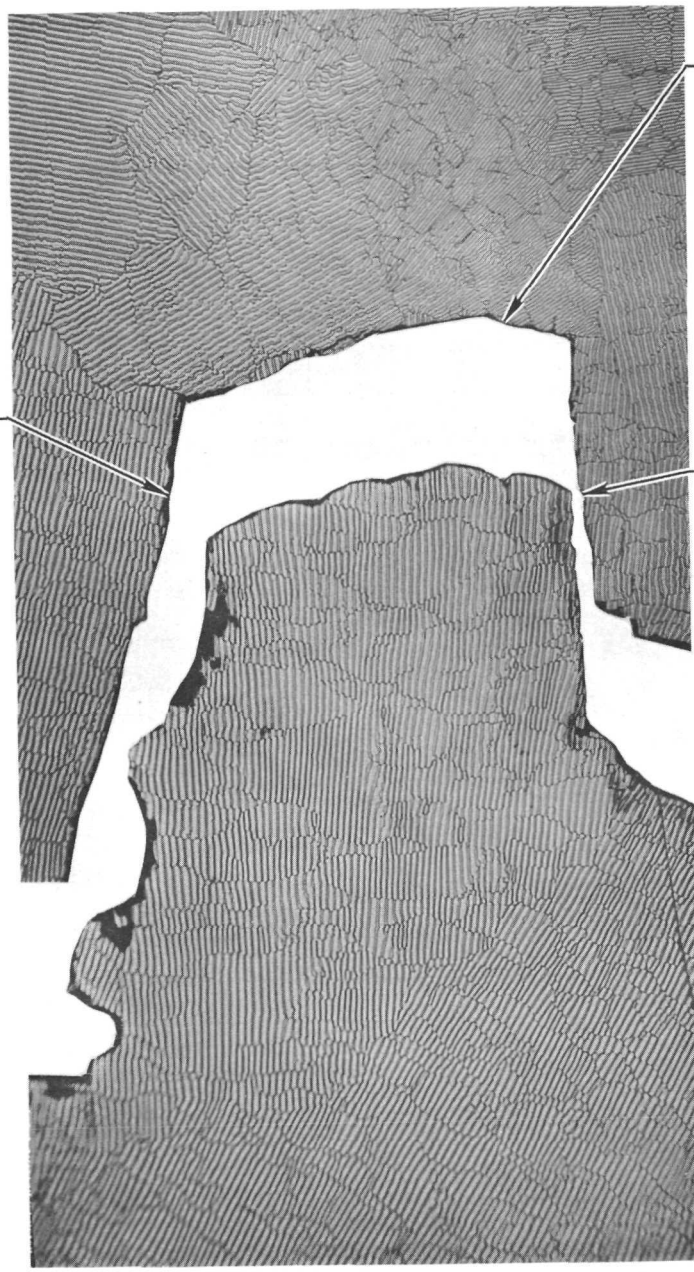

FIG. 21

LONGITUDINAL SHEAR STRESS VS DISPLACEMENT FOR Ni_3Al–Ni_3Cb EUTECTIC SOLIDIFIED AT 2 CM/HR

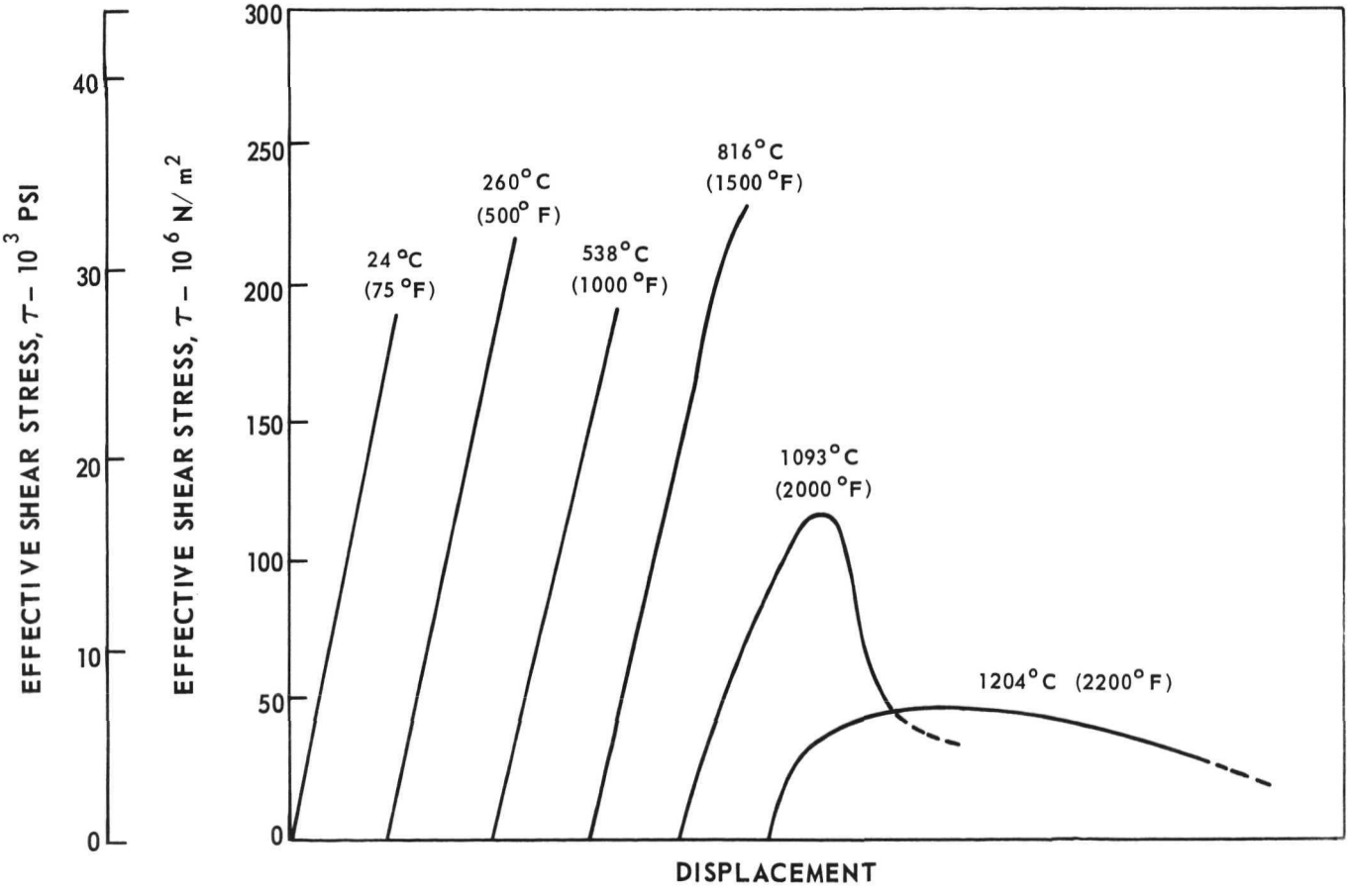

TEMPERATURE DEPENDENCE OF LONGITUDINAL SHEAR STRENGTH OF (Co,Cr,Al)–$(Cr,Co)_7C_3$ EUTECTIC SOLIDIFIED AT 10 CM/HR

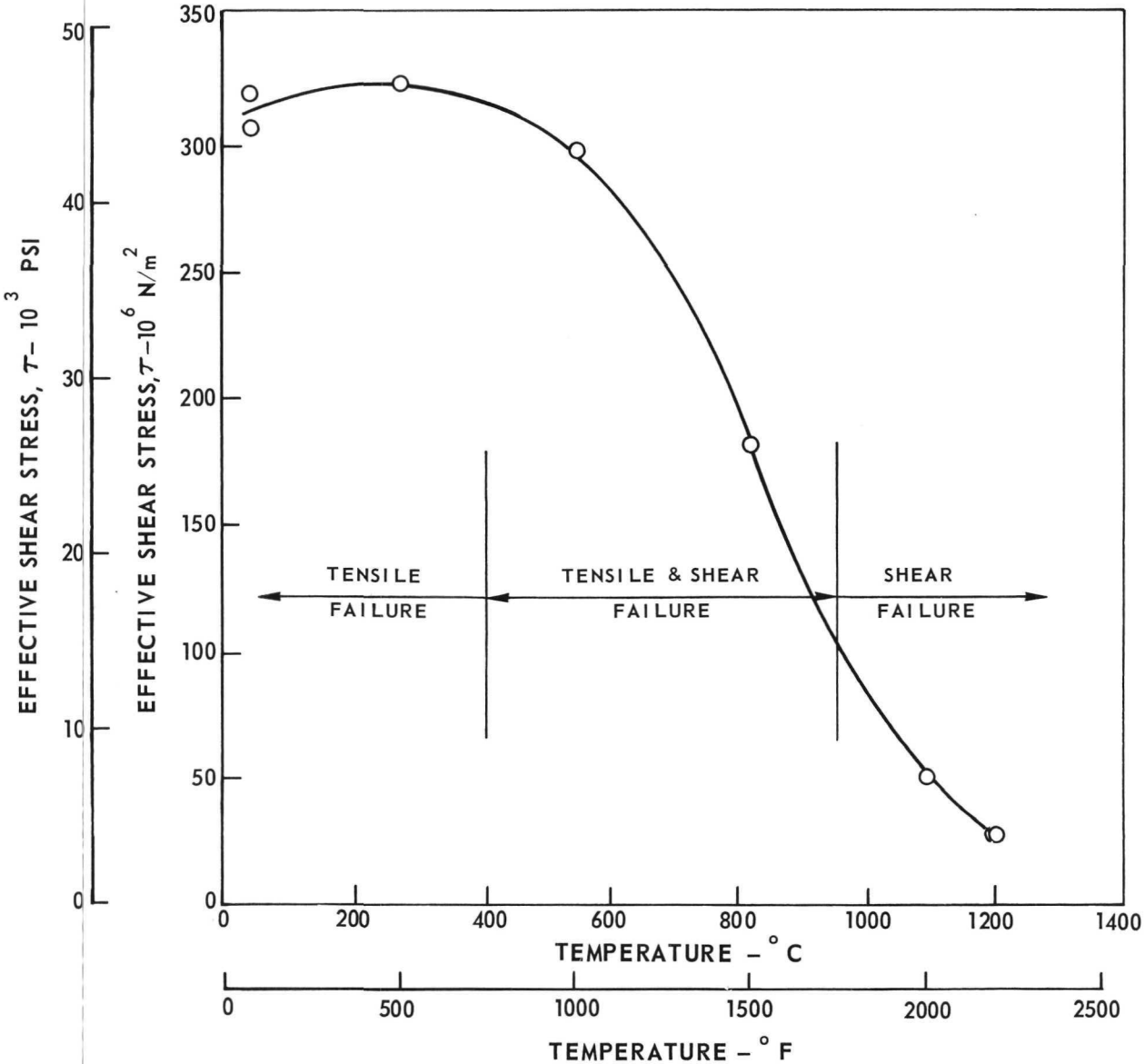

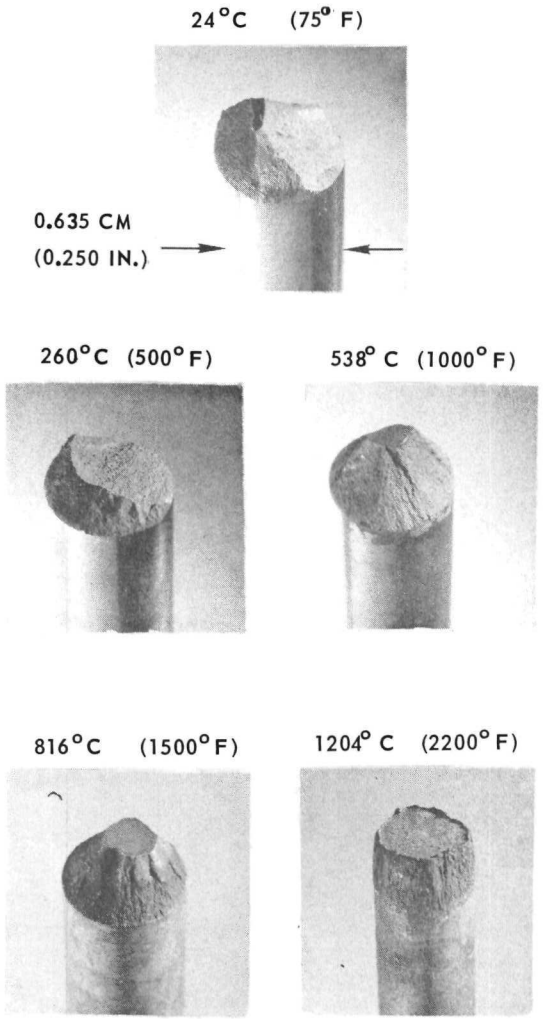

L91174-11

FIG. 22

FIG. 23

LONGITUDINAL SHEAR STRESS VS DISPLACEMENT FOR $(Co, Cr, Al)-(Cr, Co)_7C_3$ EUTECTIC SOLIDIFIED AT 10 CM/HR

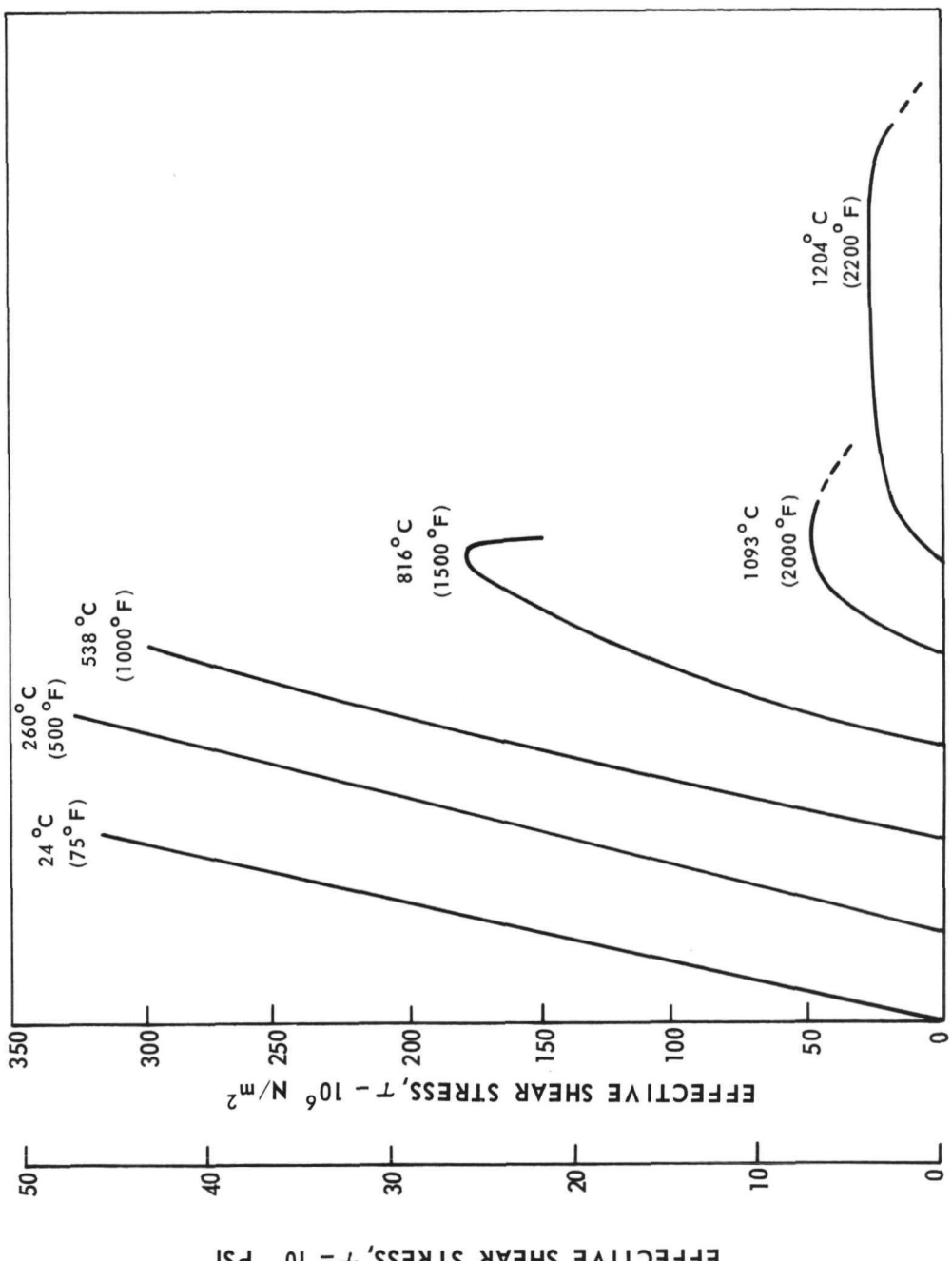

LONGITUDINAL SHEAR STRESS VS DISPLACEMENT FOR (Co, Cr, Al) – $(Cr, Co)_7 C_3$ EUTECTIC SOLIDIFIED AT 10 CM/HR

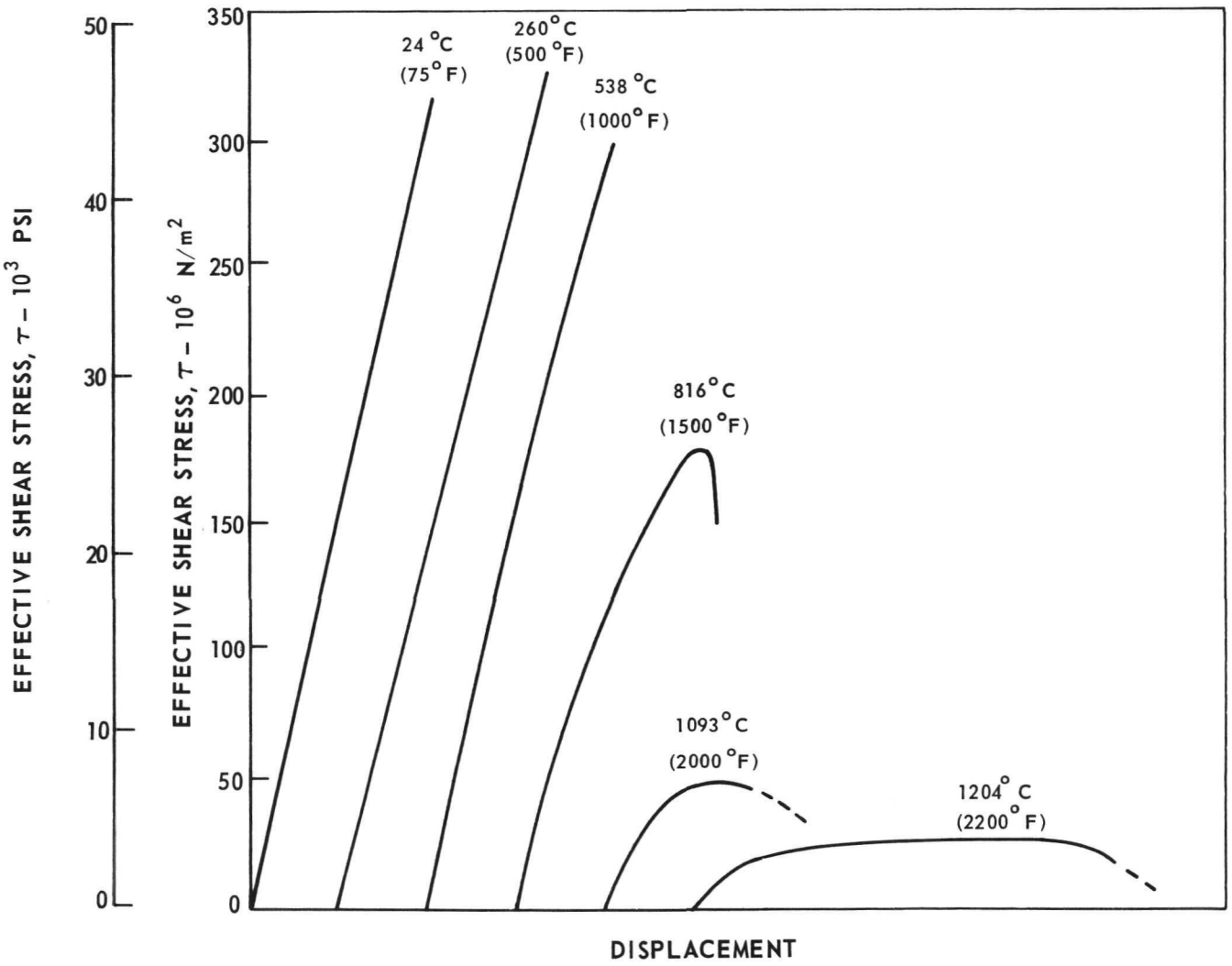

FIG. 23

FIG. 24

TEMPERATURE DEPENDENCE OF LONGITUDINAL THREAD SHEAR STRENGTH

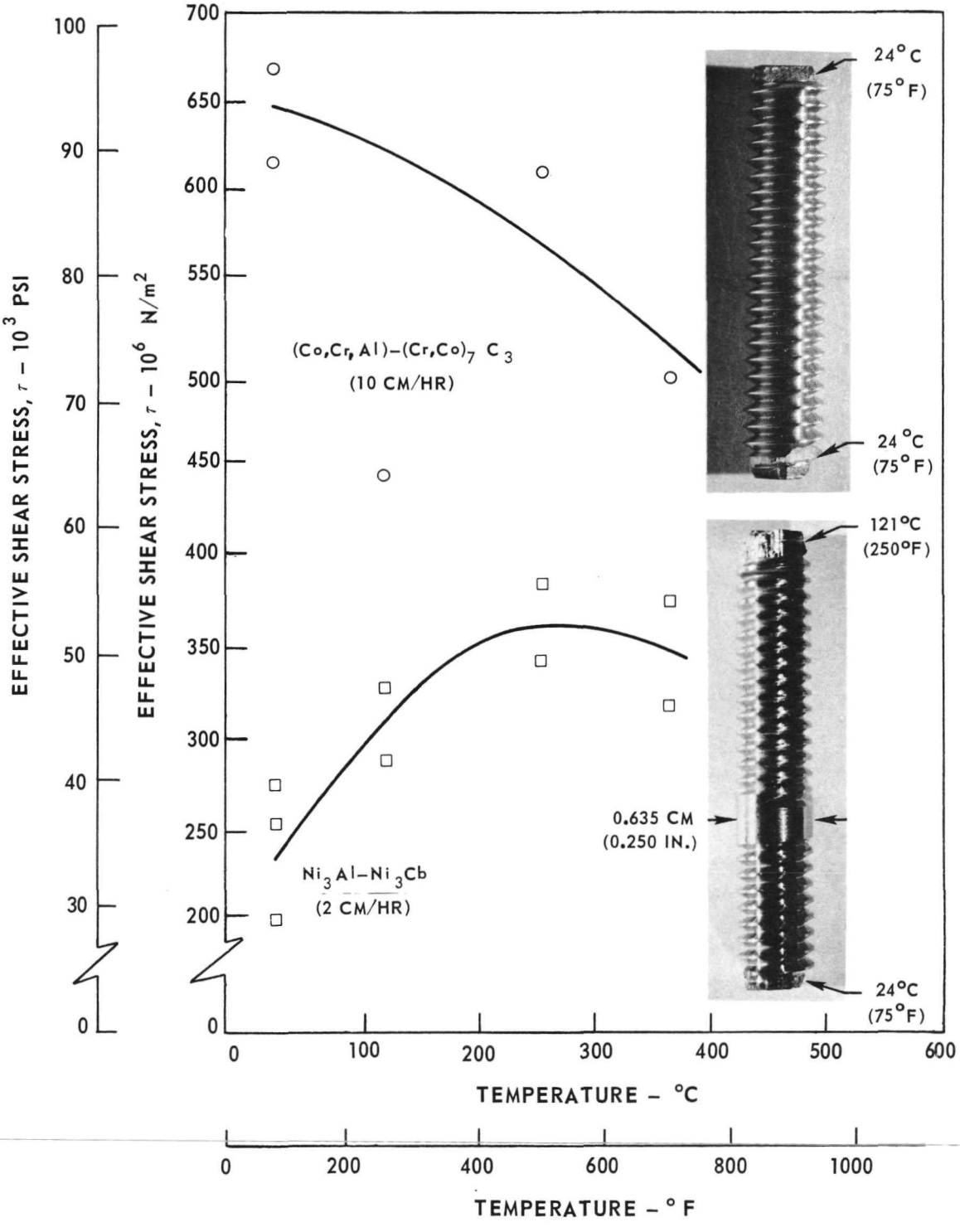

L911174-11

TORQUE VS ANGLE OF TWIST FOR Ni_3Al–Ni_3Cb EUTECTIC SOLIDIFIED AT 2 cm/hr

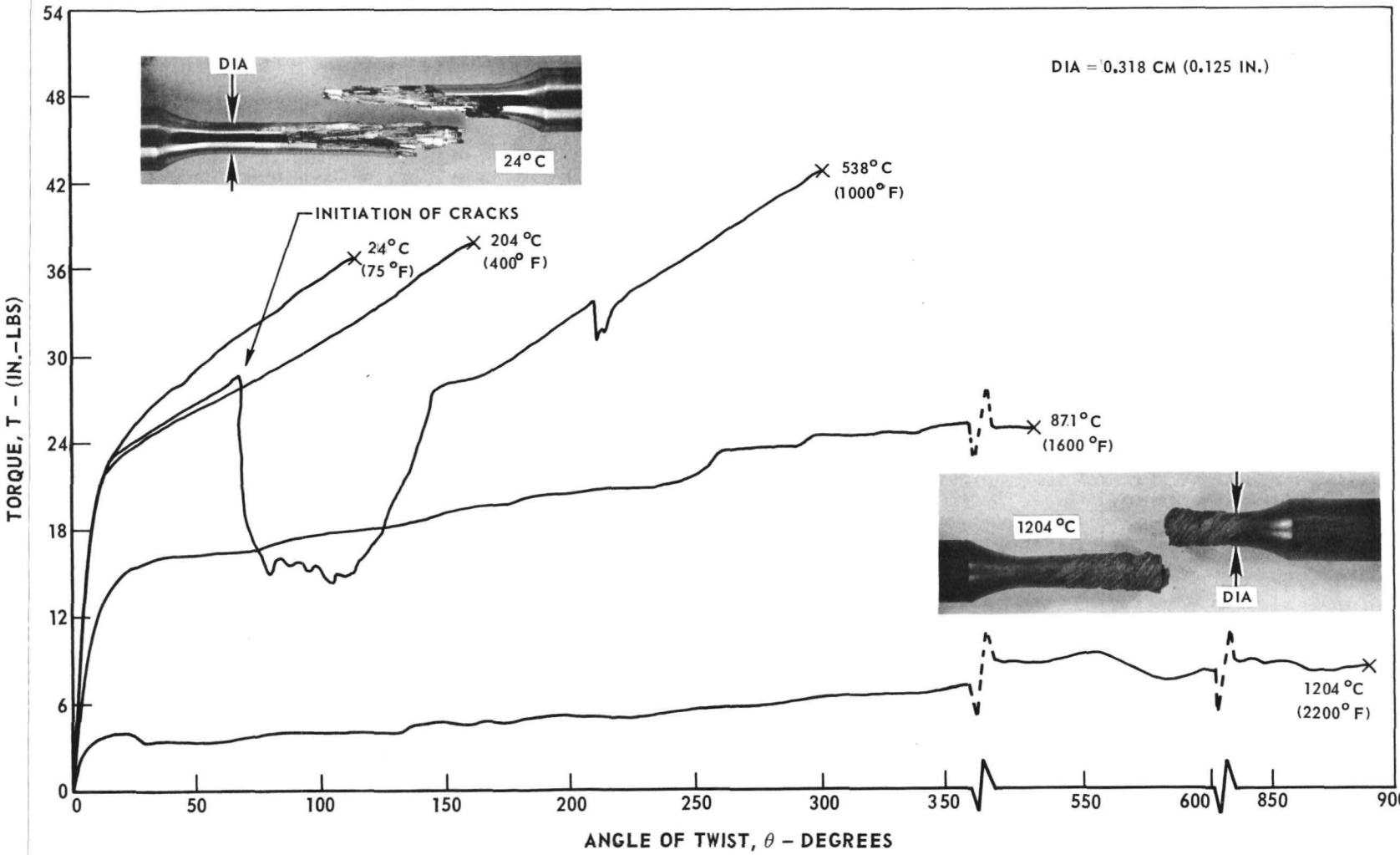

FIG. 25

TORQUE VS ANGLE OF TWIST FOR (Co, Cr, Al) – $(Cr, Co)_7 C_3$ EUTECTIC SOLIDIFIED AT 10 cm/hr

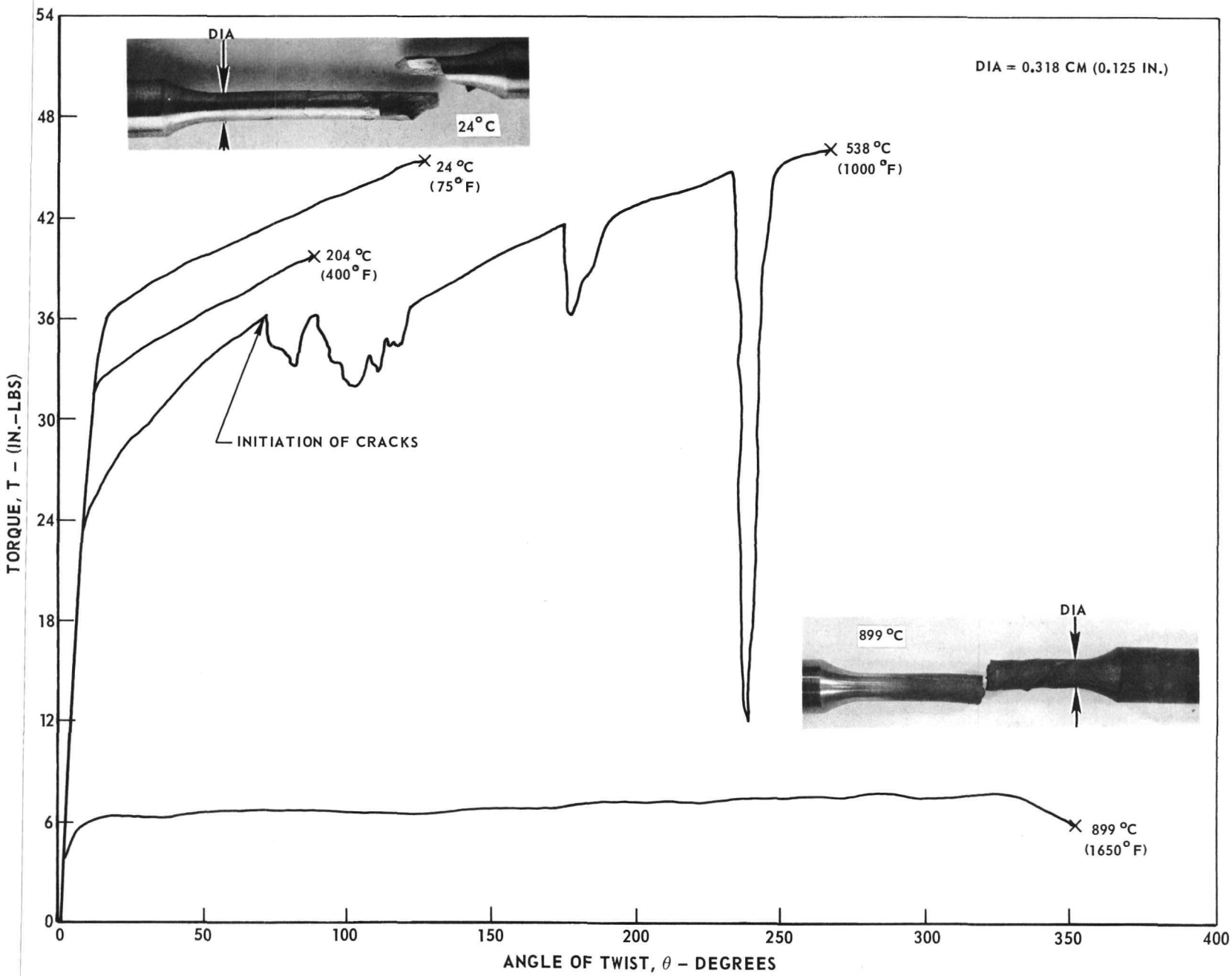

L911174-11

FIG. 26

L911174-11

GROUND FLUSH HEAD FASTENER SHAPE OF Ni_3Al–Ni_3Cb EUTECTIC SOLIDIFIED AT 2 cm/hr

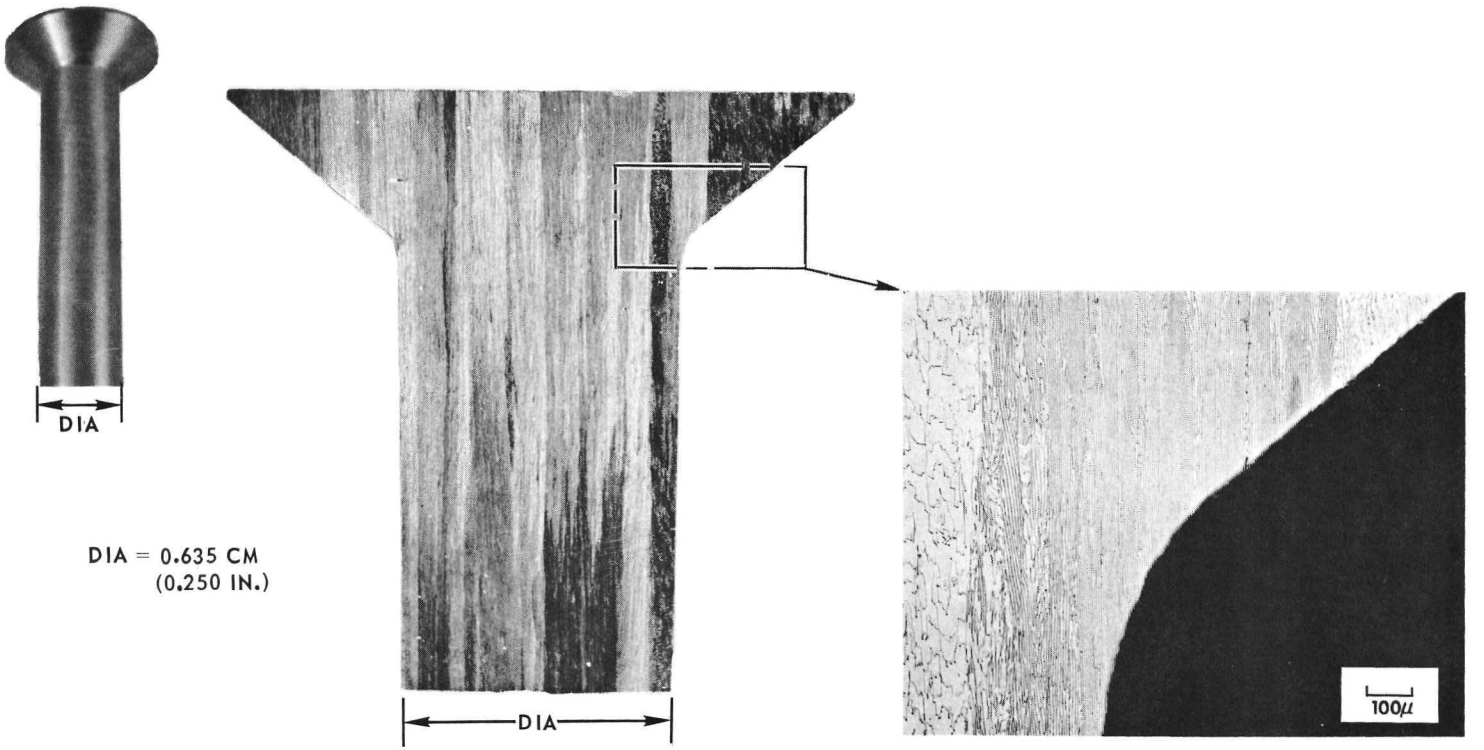

DIA = 0.635 CM
(0.250 IN.)

FIG. 27

CAST SINGLE FLUSH HEAD FASTENER SHAPES OF Ni_3Al–Ni_3Cb EUTECTIC SOLIDIFIED AT 2 cm/hr

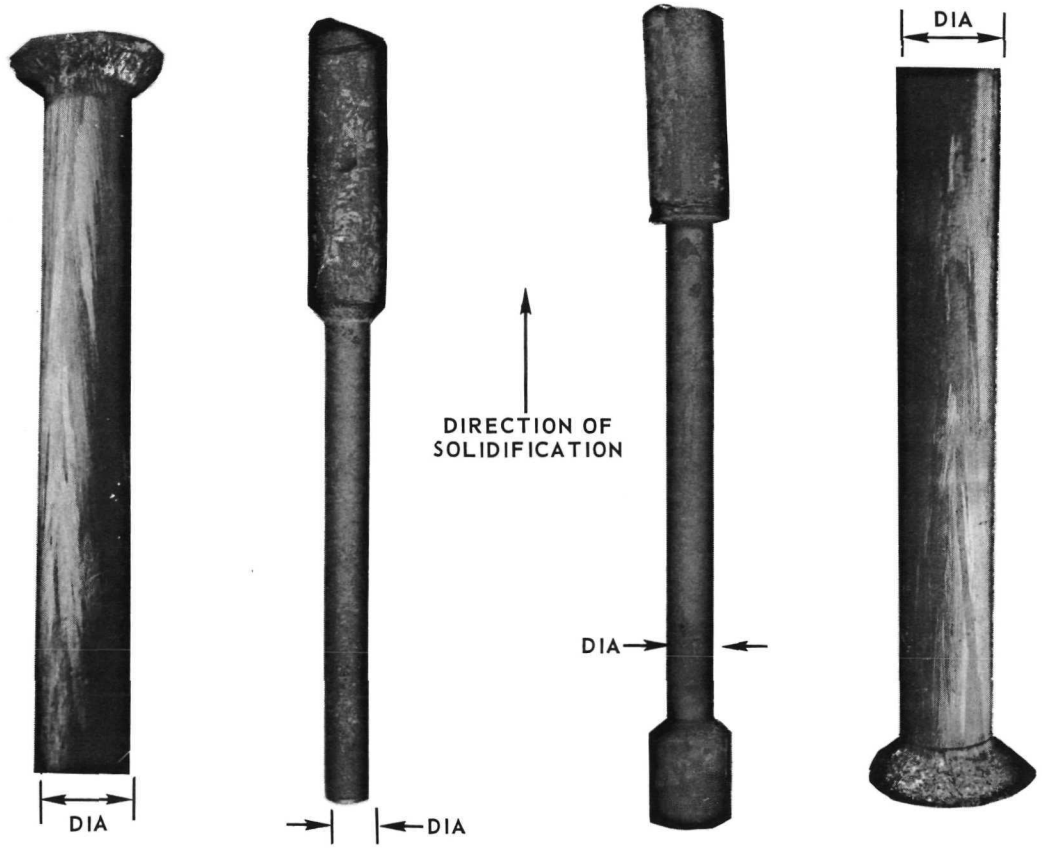

DIA = 0.635 CM
(0.250 IN.)

CAST DOUBLE FLUSH HEAD FASTENER SHAPE OF Ni_3Al–Ni_3Cb EUTECTIC SOLIDIFIED AT 2 cm/hr

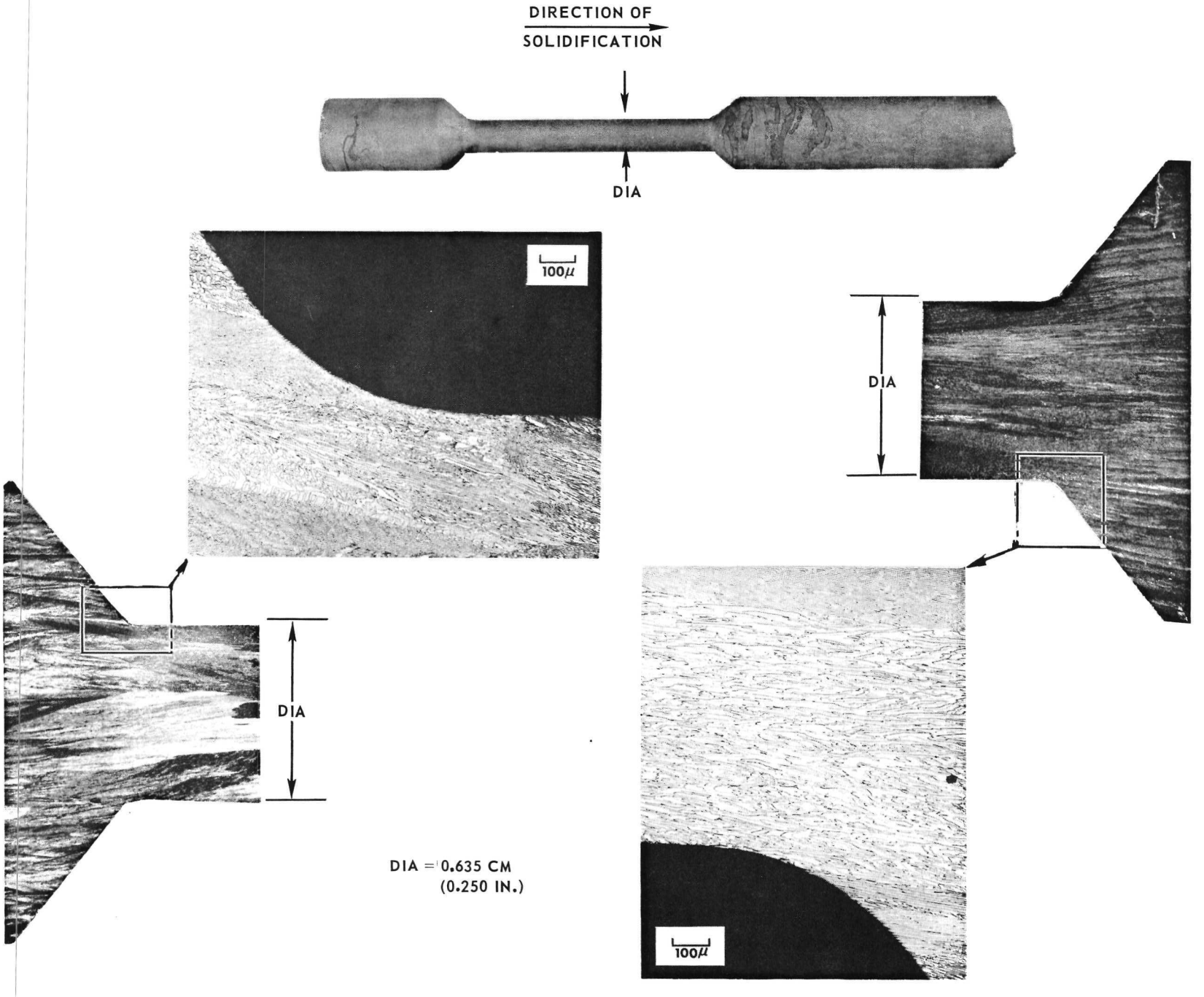

DIA = 0.635 CM
(0.250 IN.)

L911174-11

FIG. 29

CREEP FORMED FLUSH HEAD FASTENER SHAPE OF Ni_3Al–Ni_3Cb EUTECTIC SOLIDIFIED AT 16 CM/HR

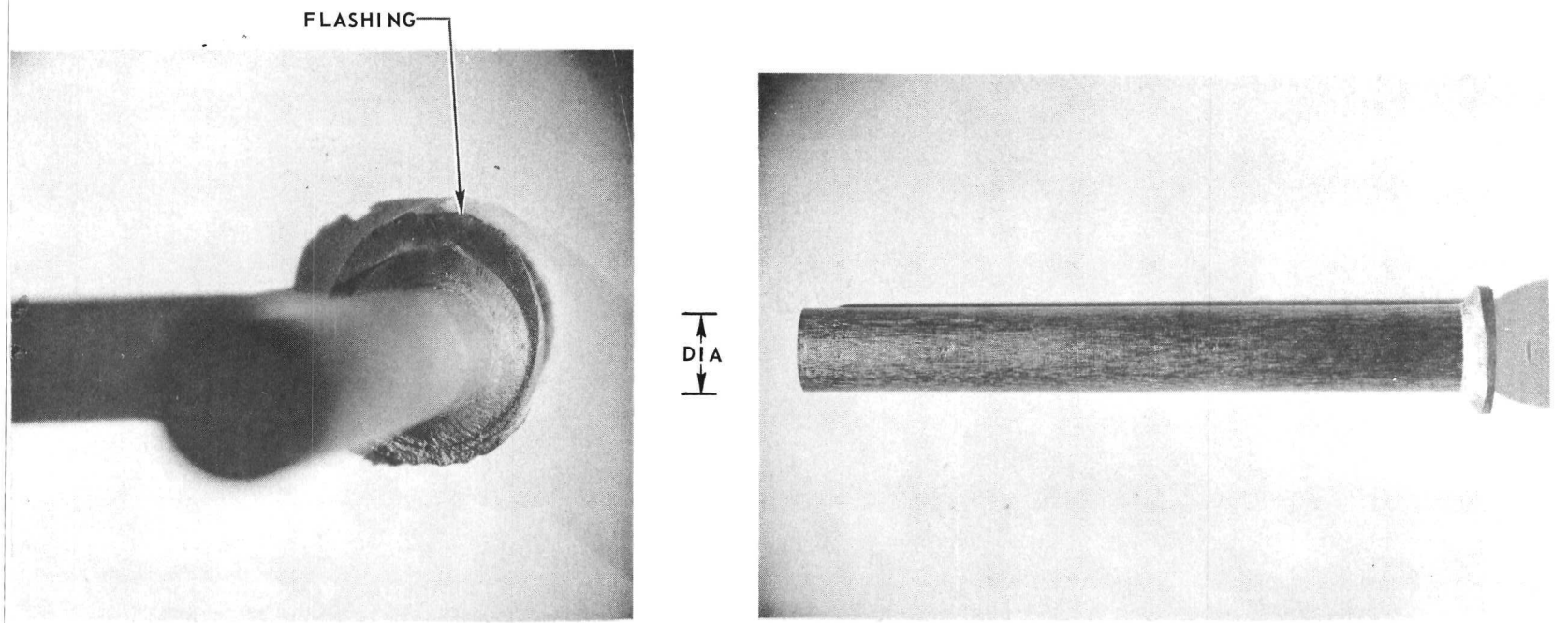

AS FORMED – WITH FLASHING AROUND FASTENER HEAD

AFTER GRINDING HEAD AND MACRO-ETCHING FASTENER SURFACE

DIA = 0.635 CM (0.250 IN.)

L911174-11

CREEP FORMED FLUSH HEAD FASTENER SHAPE OF Ni_3Al–Ni_3Cb EUTECTIC
SOLIDIFIED AT 2 cm/hr

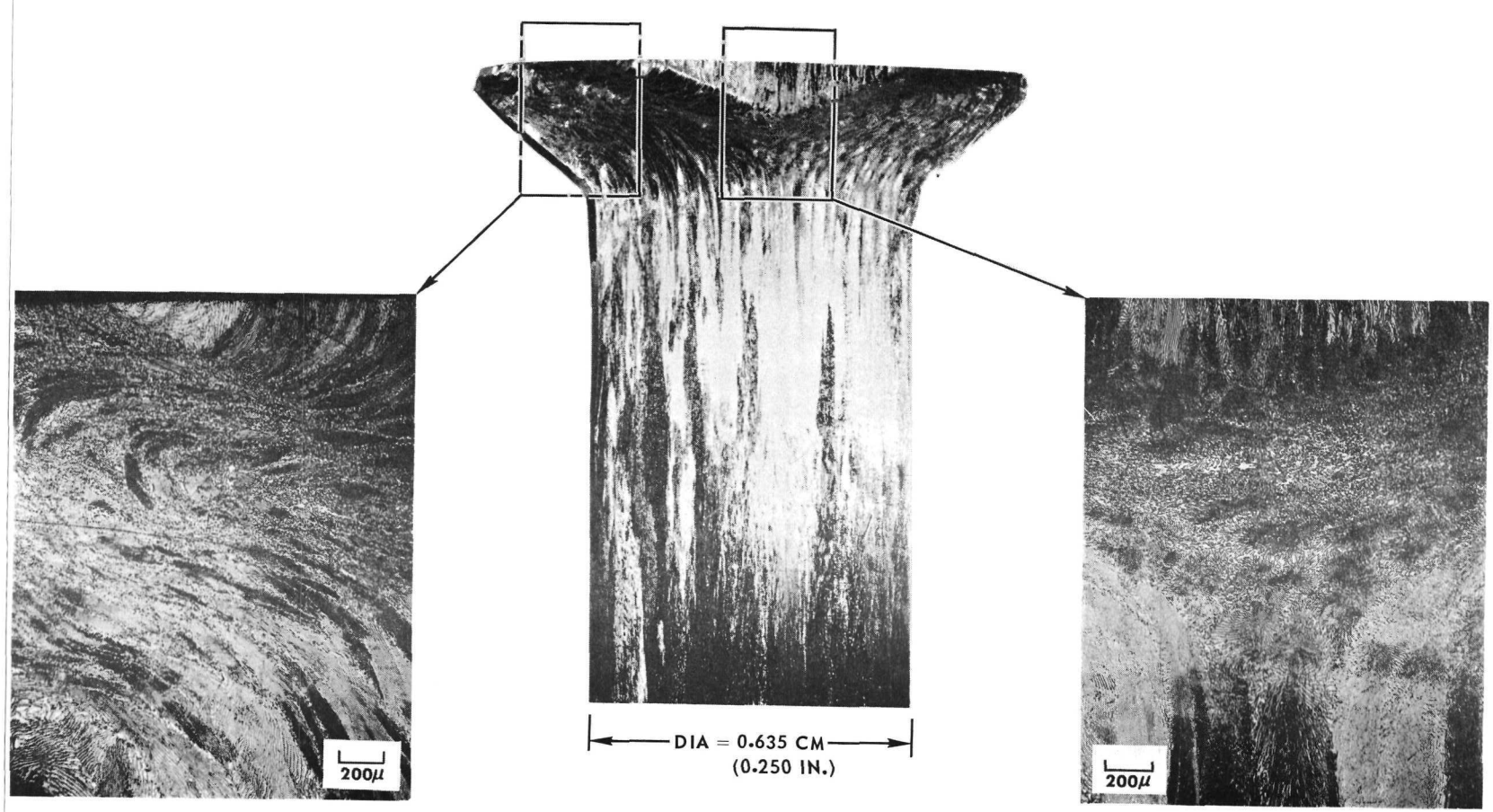

FIG. 31

L911174-11

CREEP FORMED FLUSH HEAD FASTENER SHAPE OF (Co,Cr,Al)–$(Cr,Co)_7C_3$ EUTECTIC SOLIDIFIED AT 10 cm/hr

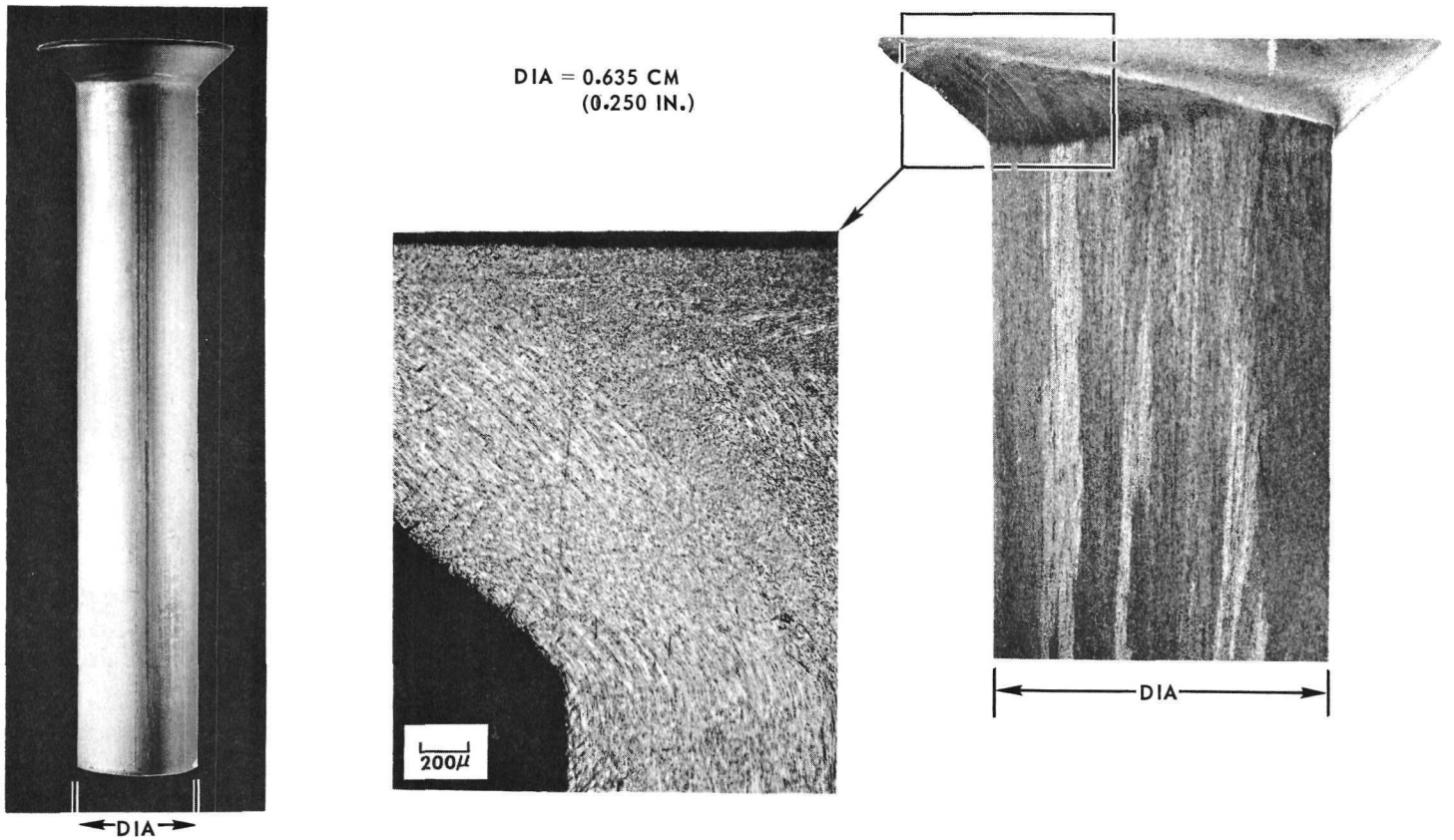

FIG. 32

ROOM TEMPERATURE SHEAR STRENGTH EVALUATION OF GROUND FASTENER SHAPES OF Ni_3Al–Ni_3Cb EUTECTIC SOLIDIFIED AT 2 CM/HR

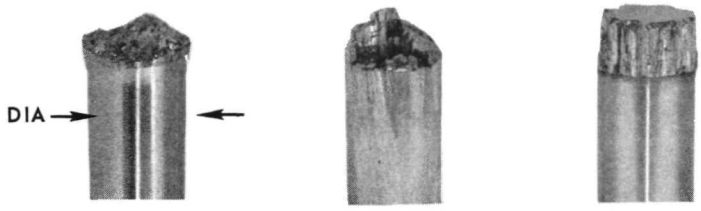

DIA = 0.635 CM (0.250 IN.)

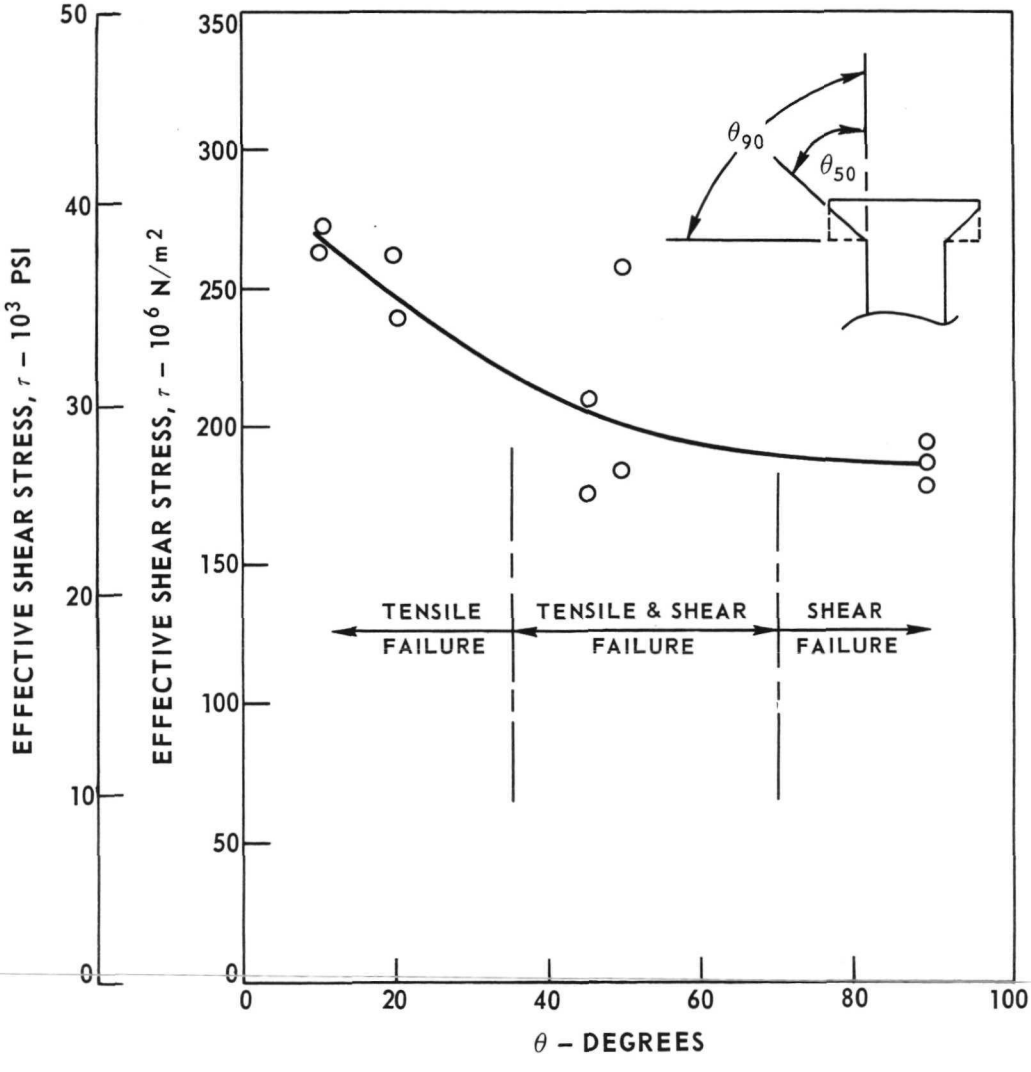

FIG. 34

STRESS-RUPTURE LIFE VS STRESS AT 2000 °F